Thesis for the Degree of Doctor of Philosophy

Millimeter Wave Slot Array Antennas based on Gap Waveguide Technology

Jinlin Liu

CHALMERS

Department of Electrical Engineering
Chalmers University of Technology

Göteborg, Sweden 2019

Millimeter Wave Slot Array Antennas based on Gap Waveguide Technology

Jinlin Liu

ISBN 978-91-7905-177-8

Doktorsavhandlingar vid Chalmers tekniska högskola
Ny serie nr 4644
ISSN 0346-718X

Department of Electrical Engineering
Division of Communications and Antenna Systems
Chalmers University of Technology
SE–412 96 Göteborg
Sweden
Telephone: +46 (0)31 – 772 1000
Email: jinlin.liu@chalmers.se

Typeset by the author using LaTeX.

Chalmers Reproservice
Göteborg, Sweden 2019

To my family

"Look deep into nature, and then you will understand everything better"
-Albert Einstein

Abstract

Recently, gap waveguide technology is introduced as a promising guiding structure for millimeter-wave systems. The conception of gap waveguide technology can be modeled for theoretical analysis by two parallel plates, a top perfect electric conductor layer and a bottom perfect magnetic conductor layer. This structure stops all modes propagating in all directions except for a quasi-TEM mode along the strip over a specific frequency band (stopband) when the gap between PEC and PMC plates is smaller than quarter wavelength at an operation frequency. Until now there are already four different versions of this novel concept—groove, ridge, inverted microstrip and microstrip ridge gap waveguides. The proposed thesis mainly focuses on array antenna design based on gap waveguide technology. We present several low-profile single-layered and multilayer corporate-fed slot array antennas with high gain for the 60-GHz band and 140-GHz. The aim of this thesis is to demonstrate the advantages of gap waveguide technology as an alternative to the traditional low-loss waveguide structure to overcome the problem of good electrical contact due to mechanical assembly. Measurement results and experimental validation are provided for the presented antenna design.

Keywords: metallic pins, perfect magnetic conductor, inverted microstrip gap waveguide, ridge gap waveguide, slots array antenna, 60-GHz and 140-GHz.

Preface

This thesis is in partial fulfillment for the Doctor of Philosophy at Chalmers University of Technology.

The work that has resulted in this thesis was carried out between September 2014 and July 2019 and has been performed within the Division of Communications and Antennas Systems at the Department of Electrical Engineering, Chalmers University of Technology. Professor Jian Yang has been the examiner, and Associate Professor Ashraf Uz Zaman has been the main supervisor.

This work is financially supported by the Swedish Governmental Agency for Innovation Systems VINNOVA via a project within the VINN Excellence center CHASE and the European Research Council (ERC) under 7th Framework Program ERC grant number 3222804.

Acknowledgments

First of all, I would like to thank Prof.Per-Simon Kildal for giving me the opportunity to work on gap waveguide technology. His leaving is irreversibly loss in the antenna world. I would like to thank head of the group Prof.Marianna Ivashina and my examiner Prof.Jian Yang for the humanization management and kind guidance to work on challenging and relevant research topics. I also would like to thank my main supervisor Associate Prof.Ashraf Uz Zaman for his selection working in the group, constructive feedbacks and kind supervision of the project. His fruitful knowledges in gap waveguide and slot array antennas helped me in the design and manufacture of slot array antennas. I would like to express my appreciation to Associate Prof.Rob Maaskant, Associate Prof.Andreas Alayon Glazunov and Assistant Prof.Simon Zhongxia He for their encouragements in research and study during these years. Furthermore, I would like to appreciate Prof.Anja Skrivervik at EPFL, Prof.Daniel Sjoeberg at Lund Univeristy, Associate Prof.Pablo Padilla, Dr.Anders Hoeoek from SAAB and Prof.Thomas Rylander for their work on my Ph.D defense during their busy time schedules.

Furthermore, I would like to express my gratitude to every member in antenna group for the perfect research and work environment. First of all, I am very grateful for my former officemate Dr.Abbas Vosoogh, who is not only a microwave and antenna scientist and engineer, but also an artist for his creative ideas and highly efficient work in the fields of gap waveguide antennas, packagings and even wireless link systems. It makes research simple and highly efficient to collaborate with him. Then I would like to thank Dr.Carlo Bencivenni for his kind help and encouragement in the group. Many thanks to Dr.Sadegh Mansouri Moghaddam for his helpful advices and discussions in research and study in the group. Then I appreciate Dr.Astrid Algaba Brazalez at Ericsson for her pioneer work on the transition design of inverted microstrip gap waveguide and delicious Jamon iberico from Spain. Then I am very grateful to Dr.Aidin Razavi, Madeleine Schilliger Kildal, Wan-Chun Liao and Jonas Flygare for their kind discussions in antennas, microwave engineering and softwares. Then I would like to thank Artem Roev, Dr.Oleg Iupikov, Dr.Abolfazl Haddadi, Parastoo Taghikhani, Navid Amani, Samar Hosseinzadegan, Morteza Ghaderi Aram, Massimiliano Zanoli, Alhasssan Aljarosha, Prabhat Khanal and Dr. Cristina Rigato for their getting along with in the department. Then I am very grateful to Chinese

friends Chao Fang, Hao Guo, and Xinxin Yang for their help in the study and life in Sweden.

My special thanks go to all the former and current secretaries of the Electrical Engineering Department for creating a nice and enjoyable working environment. We have had a lot of fun and enjoyable moments both at work and afterwork time.

Jinlin Liu

List of Publications

This thesis is based on the work contained in the following appended papers:

Paper 1
J. Liu, A. Vosoogh, A. U. Zaman, and Jian Yang, "Design and Fabrication of a High Gain 60-GHz Cavity-backed Slot Antenna Array fed by Inverted Microstrip Gap Waveguide", *IEEE Transactions on Antennas and Propagation*, vol. 65, no. 4, pp. 2117-2122, April, 2017.

Paper 2
J. Liu, Jian Yang, and A. U. Zaman, "Analytical Solutions towards Inverted Microstrip Gap Waveguide for characteristic Impedance and Losses based on variational Method", *IEEE Transactions on Antennas and Propagation*, vol. 66, no. 12, pp. 7049-7057, December, 2018.

Paper 3
J. Liu, A. Vosoogh, A. U. Zaman, and Jian Yang, "A Slot Array Antenna With Single-Layered Corporate-Feed Based on Ridge Gap Waveguide in the 60-GHz Band", *IEEE Transactions on Antennas and Propagation*, vol. 67, no. 3, pp. 1650-1658, March, 2019.

Paper 4
J. Liu, A. U. Zaman, and Jian Yang, "Design and Fabrication of a High-Gain Slot Array Antenna based on Ridge Gap Waveguide at 140 GHz", submitted to *IEEE Transactions on Antennas and Propagation*.

Other Publications
Additional related publications by the Author, not included in this thesis. The content partially overlaps with the appended papers or is out of the scope of the thesis.

Paper A
J. Liu, A. Vosoogh, A. Uz Zaman and P.-S. Kildal, "Design of a Cavity-backed Slot Array Unit Cell on Inverted Microstrip Gap Waveguide", *Antennas and Propagation*

(ISAP), 2015 International Symposium on, 24-28, October, 2015.

Paper B
J. Liu, A. Uz Zaman and P.-S. Kildal, "Optimizing the numerical port for inverted microstrip gap waveguide in full-wave simulators",*Antennas and Propagation (EUCAP), Proceedings of the 10th European Conference on*, 10-15, April, 2016.

Paper C
J. Liu, A. Uz Zaman and P.-S. Kildal, "Design of transition from WR-15 to inverted microstrip gap waveguide, "*2016 Global Symposium on Millimeter Waves (GSMM) Technology and Applications*, 6-8, June, 2016.

Paper D
J. Liu, A. Vosoogh, A. Uz Zaman and P.-S. Kildal, "Design of 8 ×8 slot array antenna based on inverted microstrip gap waveguide, "*Antennas and Propagation (ISAP), 2016 International Symposium on*, 24-28, October, 2016.

Paper E
J. Liu, A. Vosoogh, A. Uz Zaman and Jian Yang, "A High-Gain High-Efficiency Corporate-Fed Slot Array Antenna directly Fed by Ridge Gap Waveguide at 60-GHz, "*Antennas and Propagation (ISAP), 2017 International Symposium on*, 27-30, October, 2017. Best Paper Award 1st place

Paper F
J. Liu, A. Vosoogh, A. Uz Zaman and Jian Yang, "Slot Antenna Array Unit Cell Directly Fed by Inverted Microstrip Gap Waveguide, "*Antennas and Propagation (ISAP), 2017 International Symposium on*, 27-30, October, 2017.

Paper G
J. Liu, A. Uz Zaman and Jian Yang, "Design of A Wideband Array Antenna Prototype with Gap Waveguide for W-Band Wireless Links, "*Antennas and Propagation (EUCAP), Proceedings of the 12th European Conference on*, 8-12, April, 2018.

Paper H
J. Liu, A. Uz Zaman and Jian Yang, "Comparison among Microstrip, Covered Microstrip and Inverted Microstrip Gap Waveguide in Losses based on Variational Method in Millimeter Waves "*Swedish Microwave Days 2018*, 8th, July, 2018.

Paper I
J. Liu, A. Uz Zaman and Jian Yang, "Design of Wideband Slot Array Antenna by Groove Gap Waveguide in Millimeter Waves, "*IEEE-APS Topical Conference on Antennas and Propagation in Wireless Communications (APWC)*, 10-14, September, 2018.

Paper J
J. Liu, A. Uz Zaman and Jian Yang, "Study of Dielectric Loss and Conductor Loss among Microstrip, Covered Microstrip and Inverted Microstrip Gap Waveguide Utilizing Variational Method in Millimeter Waves, " *Antennas and Propagation (ISAP), 2018 International Symposium on*, 24-28, October, 2018.

Paper K
J. Liu, A. Uz Zaman and Jian Yang, "Design of a 32 by 32 Slot Array Antenna based on Ridge Gap Waveguide at 140 GHz, " *The Cross Strait Quad-Regional Radio Science and Wireless Technology Conference*, 18-22, July, 2019.

Paper L
J. Liu, A. Uz Zaman and Jian Yang, "Two Types of High Gain Slot Array Antennas based on Ridge Gap Waveguide in the D-Band, " *IEEE-APS Topical Conference on Antennas and Propagation in Wireless Communications (APWC)*, 12-16, September, 2019.

Paper M
J. Liu, A. Uz Zaman and Jian Yang, "Low sidelobe Slot Array Antenna based on Inverted Microstrip Gap Waveguide at 28 GHz, " *Antennas and Propagation (ISAP), 2019 International Symposium on*, 28-31, October, 2019.

Paper N
J. Liu, A. Uz Zaman and Jian Yang, "Double-layer corporate-fed Slot Array Antenna with Taylor-Distribution Synthesis by unequal Power Divider based on Inverted Microstrip Gap Waveguide at Ka-Band, to be submitted to *IEEE Transactions on Antennas and Propagation*, 2019.

Contents

Part I

Introductory Chapters

Chapter 1

Introduction

Communication technology has developed so fast in the past half century. In general, the communication technology has a profound influences in the modern society. Today coordination and knowledge among people are facilitated by the rapid advancement of wireless and mobile communications. Wi-Fi and base station networks are now spread almost everywhere allowing people to access anytime with the mobile terminals. In 2020 the number of users will be exceeding five billion and expected to rise even more in the next decades. Potential commercial applications for wireless system include point to multi-point services, chip to chip high speed links, satellite communications, automotive radars, imaging and security systems. However, the current saturation of spectrum at microwave frequencies below 10 GHz is the major challenge.Thereby, it is necessary to explore new frequency bands in higher frequencies. Currently, considerable attention has been paid to millimeter and sub-millimeter wave communications [1]. However, wireless communications at such frequency bands are easily affected by the propagation loss and strong atmospheric absorption according to fundamental principles of electromagnetic field theory [2]. Therefore, waveguide structures with low loss property and high gain antennas are required for such a kind of wireless systems.

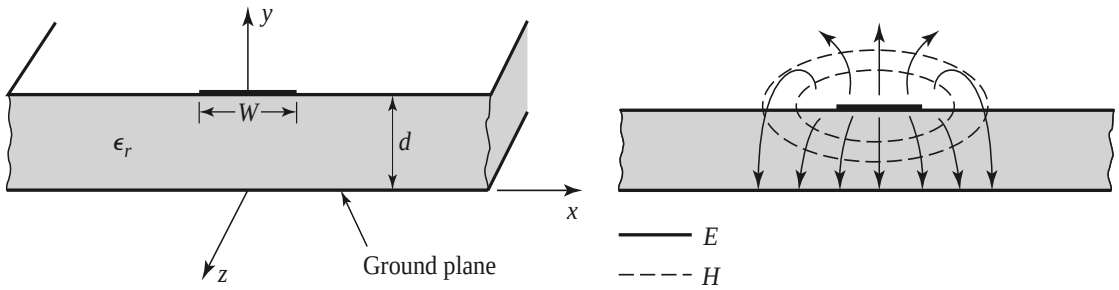

Figure 1.1: Microstrip Transmission Line.

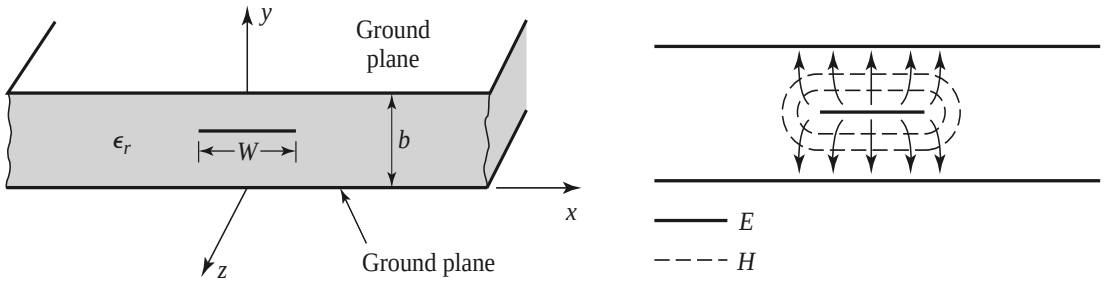

Figure 1.2: Stripline Transmission Line.

As is well-known, transmission lines are frequently utilized for traditional communications systems. Transmission lines are specialized cable structures which carry alternate current of radio frequency. In reality, transmission lines are used with the purposes such as connected circuits for transmitter, receiver and antennas, distributed television cable and high speed bus system in a computer. The most common types of transmission lines are microstrip line and stripline. A microstrip line is the most popular transmission line, as illustrated in Figure 1.1. A good conductor which is usually copper of width W is printed on a thin, grounded dielectric substrate of thickness d and relative permittivity ε_r. A regular sketch of the corresponding E- and H-fields is also shown in the Figure 1.1. Similarly, the geometry of a stripline is depicted in Figure 1.2. A thin conducting strip of width W is centered between two wide conducting ground planes of separation b, the area between the ground planes is filled with a dielectric material. In reality, stripline is usually constructed by etching the center conductor on a grounded dielectric substrate of thickness $b/2$ and then covering with another grounded substrate.

Generally, the total loss energy in a RF system consists of dielectric and conduction loss. Considering that those two wave-guided structures suffer from dielectric substrate, the dielectric loss is unavoidable in them. The stripline and the microstrip line are typical applied topologies based on parallel-plate transmission line. Theoretically, the dielectric loss can be expressed as the multiplication of the frequency and loss tangent of the materials. Therefore, the corresponding dielectric loss squarely increases against the frequency. The high dielectric loss is one of the main problems in transmission lines at millimeter wave frequency band for planar array technologies.

The waveguide structure usually refers to the rectangular and circular waveguide. A typical geometry of rectangular waveguide is depicted in Figure 1.3. The hollow waveguide characterizes high power handling capability, good isolation, large gain/high efficiency array antennas or high-Q filters. However, the fabrication cost of hollow waveguide will also be considered for millimeter wave frequency band. Until now we have several methods to fabricate waveguide structures, such as Computer-

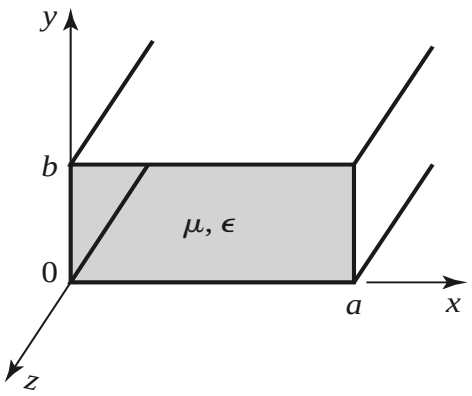

Figure 1.3: The geometry of a rectangular waveguide.

ized Numerical Control machining and Electric Discharging Machining. Generally, the waveguide structures are typically manufactured in split-blocks and then be connected by screwing, diffusion bonding or deep-brazing techniques. In millimeter wave band the split-blocks are very small so that the manufacture outcomes usually are not accurate and perfect.

Substrate integrated waveguide (SIW) [3] has shown big advantages over both standard rectangular waveguide and printed circuit based transmission lines in millimeter waves. Geometrically, SIW is a compact planar printed circuit in which two rows of metallic via holes are embedded within a substrate material between two metallic plates, as illustrated in Figure 1.4. The electromagnetic behaviors of SIW is similar to those of rectangular waveguides with filled dielectrics [4]. The difference existing is that the electromagnetic wave propagates between two rows of metallic via holes instead of metallic walls in rectangular waveguide. Until now, various array antennas fed by SIW distribution networks have been reported in [5–12]. Moreover,

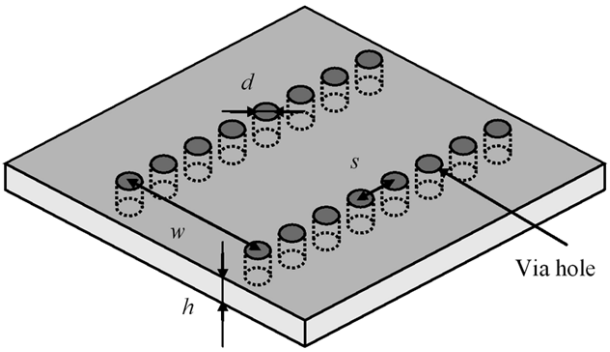

Figure 1.4: The geometry of a rectangular waveguide.

SIW has an outstanding profile which facilities its easy integration with active RF components, such as low noise amplifier, power amplifier and mixer [13]. Nevertheless, SIW still has dielectric loss like normal microstrip lines due to the use of the substrate [14]. Applying low loss substrate materials is a choice to fabricate the SIW structure, but the dielectric loss still exists and its cost might increase. Another critical point to the overall loss in SIW is the leakage energy through the gaps between metallic via holes when these are not properly organized [15]. Thereby, the dimensions of metallic via holes, the periodic space and the contact between two plates might increase the design complexity and the cost.

The recently introduced gap waveguide technology [16] constitutes a new type of wave guiding structure which presents lots of potential to overcome the problems existing in conventional technologies mentioned before. The newly proposed gap waveguide technology is based on the research results of soft- and hard- surfaces [17], which states the cutoff of electromagnetic fields when a metal plate is placed parallel to a textured artificial magnetic conductor (AMC) and their distance is smaller than quarter wavelength. The AMC surface is able to establish a high impedance surface boundary condition that ensures the removal of any parallel-plate mode, cavity mode, surface waves within a certain frequency band called the stopband. Usually this AMC is realized by the periodic structure by metallic pins or mushrooms. Then only a local TEM mode is allowed to propagate confined within the air gap and along

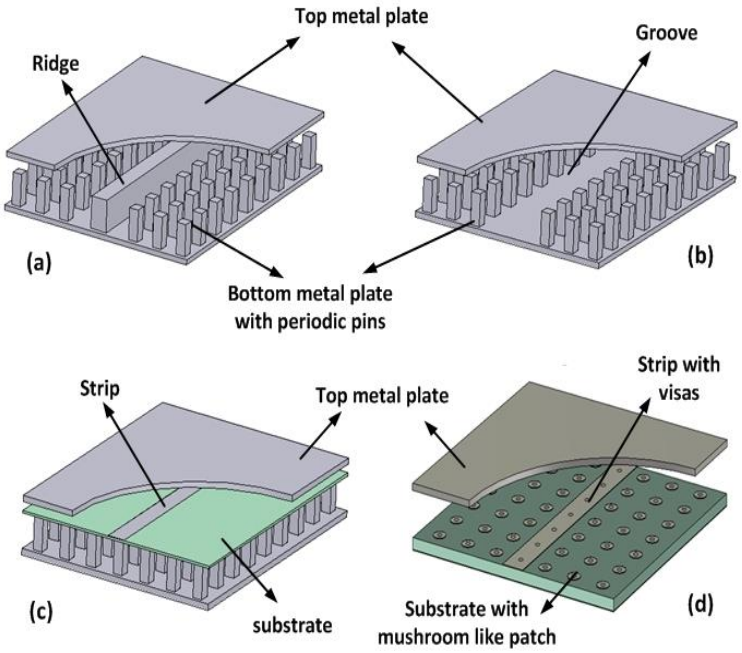

Figure 1.5: Four realized different gap waveguide geometries. (a) Ridge Gap Waveguide. (b) Groove Gap Waveguide. (c) Inverted Microstrip Gap Waveguide. (d) Microstrip-Ridged Gap Waveguide.

a desired path defined by a metallic ridge, groove or microstrip embedded in the AMC layer. Therefore, the gap waveguide technology is able to control the wave propagation in the desired paths, and forbids propagation of waves in undesired directions. Thereby, the gap waveguide technology is a promising wave guiding structure alternative to counteract the limitations of conventional technologies mentioned before in this report. So far there are four different realized versions based on guiding-line, propagation characteristics and the band gap structure. Ridge gap waveguide, groove gap waveguide, inverted microstrip gap waveguide [18] and microstrip-ridge gap waveguide [19] are four different varieties of gap waveguide technology, as depicted in Figure 1.5. Firstly, the ridge gap waveguide guides a quasi-TEM mode along the metallic ridge surrounding by metallic pins and no dielectric is required in the structure. Then the inverted microstrip gap waveguide guides a quasi-TEM mode along a microstrip etched on a Printed Circuited Broad (PCB). This PCB can be either supported by an AMC surface or AMC itself embedded in the substrate materials. In inverted microstrip gap waveguide the field is mainly confined in the air gap. The groove gap waveguide can propagate a TE_{10} mode along the periodic pins surface. No substrate material is involved in the geometry. This cutoff principle on which this new technology is based, provides promising opportunities compared to the conventional approaches, such as microstrip, coplanar waveguide, and standard waveguides. The gap waveguide technology has interesting characteristics such as low loss [18], easy manufacturing [20], and cost-effective RF integration [21] in millimeter wave frequencies. The advantage compared with other candidates is low loss because the wave propagates in the air. Secondly, the ridge and groove gap waveguide does not contain any dielectrics so that they can totally avoid the dielectric loss. Furthermore, they are mechanically more flexible to fabricate and assemble them than normal hollow waveguide. In addition, electrical contact between the building blocks is not needed anymore in such kinds of novel structures [22]. Thereby, this advantage offers good opportunities for making millimeter wave antennas and corporate feed networks [23–33]. And most importantly, gap waveguides geometries can be manufactured by the usage of low cost fabrication techniques such as injection molding, die pressing, plastic hot embossing or electrical discharging machining.

Another useful advantage of gap waveguide technology is that the metallic pins are able to supply PMC boundary condition. This boundary condition is able to avoid the surface current which is the origin for the metallic loss. This huge advantage can be utilized to package the integrated circuits [34–37] and passive elements [38–41]. Microstrips and coplanar waveguide transmission lines are open structures and the final products need to be protected from interference and physical damages. The traditional method is based on using metallic shielding boxes. As we discussed before, the metallic shielding boxes produce the surface current based on fundamental electromagnetic boundary condition. In addition, this method allows easy appearance of cavity resonance modes when two of the dimensions of the box are larger than half

wavelength. It is possible to suppress these resonances by adding absorber materials, which introduces additional losses. The new gap waveguide technology can avoid all such problems depicted in traditional method.

1.1 Goal and outline of the thesis

In previous paragraphs, some existing challenges in the millimeter wave technologies have been already discussed very detailed. There exists a big performance gap between the planar transmission lines such as microstrips, coplanar waveguide, SIW, multilayer technology and traditional hollow waveguide. One of the main current research challenges is to find a new guiding structure with flexible, low cost manufacture and low loss at the same time. Taking the millimeter wave antennas design as examples, hollow waveguide is able to realize a high efficiency antenna, but the manufacture cost are very high. Microstrip and SIW have low cost and easy manufacture, but they suffer from high loss and low efficiency. It is very difficult to combine all advantages together at the same time. Nevertheless, it is possible to utilize gap waveguide technology to cover all advantages together. In this thesis, several different planar slot array antennas based on groove gap waveguide, ridge gap waveguide and inverted microstrip gap waveguide in the V-Band, W-Band and D-Band will be introduced. In Chapter 2, a 16 $\times$ 16 slot array antenna fed by inverted microstrip gap waveguide (IMGW) in the V-Band is presented. The whole structure designed consists of radiating slots, a groove gap cavity layer, a distribution feeding network, and a transition from standard WR-15 waveguide to the IMGW. In Chapter 3, an 8 $\times$ 8 slot array antenna based on groove gap waveguide in the W-Band is proposed. This W-Band antenna has also been built by the radiation slots, the backed-cavity and the distribution networks. In Chapter 4, a single-layered corporate-fed array antenna in V-Band is proposed. In the geometry, the backed cavity layer is avoided. In Chapter 5, a double-layered corporate-fed array antenna in D-Band will be discussed. Both of the later array antennas are based on ridge gap waveguide. Above mentioned four antennas demonstrate high-gain, high-efficiency, low profile and low-cost fabrication. Thereby, those performances prove that gap waveguide technology has huge advantages than microstrip, coplanar array, SIW and standard waveguides. In the future, the gap waveguide technology will somehow replace the traditional wave-guided structures for its potential at millimeter wave frequency.

Chapter 2

High Gain 60-GHz array antenna based on Inverted Microstrip Gap Waveguide

This chapter deals with the design of high gain array antenna based on inverted microstrip gap waveguide in the V-Band. Compared with the other technologies introduced in chapter 1, gap waveguide decreases cost and complexity of fabrication process without the strict requirement of electric contact among different layers. In this chapter a high gain array antenna based on inverted microstrip gap waveguide will be detailed introduced. The whole structure based on inverted microstrip gap waveguide consists of radiating slots, groove gap cavity layer, distribution feeding network and a transition from standard WR-15 waveguide to inverted microstrip gap waveguide. The complete antenna array is designed and fabricated using Electrical Discharging Machining (EDM) technology. The measurement shows that the antenna has 16.95% bandwidth covering 54-64 GHz frequency range. The measured gain of the antenna is more than 28 dBi with the efficiency higher than 40% covering 54-64 GHz frequency range.

2.1 Introduction

The inverted microstrip gap waveguide technology is based on the presence of a thin substrate that lies over a periodic pin pattern that composes the bed of nails. This bed of nails constitutes an AMC material and the combination with the upper metal lid prohibits any wave propagation within the air gap, also in the presence of the dielectric layer. Only local waves are allowed to propagate along strips etched on this substrate. Figure 2.1 shows the basic layout of the inverted microstrip gap waveguide. As sketched in Figure 2.1, the inverted microstrip gap waveguide technology is based on the use of a thin substrate which is applied for feeding network and lies over a

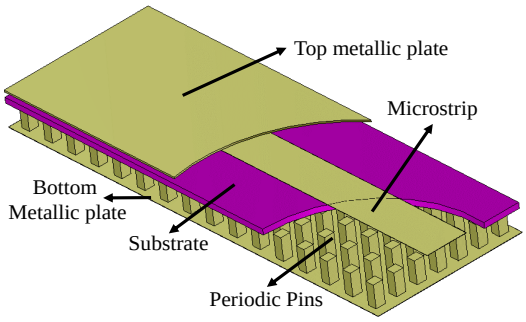

Figure 2.1: Brief geometry of the inverted microstrip gap waveguide.

periodic pin pattern. This periodic metallic pin layer constitutes an AMC surface and in combination with the upper metallic lid prohibits any wave propagation within the air gap. Furthermore, a local quasi-TEM mode is allowed to propagate along the metallic strip. The main motivation and advantage of this inverted microstrip gap waveguide antenna lies to the fact that the pin plate with uniform pin period can be easily fabricated by metal sawing or wire-cut technique and this will reduce the cost of the overall antenna. Also, the feeding network will be printed on a PCB which can be also low cost. In this chapter, we will systematically present a 16×16 slot antenna array designed with corporate feeding networks including an interface to WR-15 rectangular waveguide. The brief design idea of the complete 16×16 slot antenna array is shown as a flow chart in Figure 2.2.

2.2 Design for Bed of Nails

As mentioned in previous section, gap waveguide uses a parallel-plate stopband over a specific frequency range. The pin dimensions of bed of nails should be chosen correctly to achieve a parallel plate stopband which covers as much as 60-GHz frequency band. The basic idea is numerical parametric analysis of the inverted microstrip gap waveguide whose structure is illustrated in Figure 2.3. The PEC, periodic and PEC boundary conditions are added for the structure in x-, y- and z-axis, respectively. The geometrical parameters which effect the stopband of inverted microstrip gap waveguide are: the gap height h_g, the period p of pins, the width a of pins, the pin height h_p of pins and the thickness of substrate h_s. Here the shape of pins in XOY plane is square while dispersion diagrams metallic strip are supposed to be identical in the both propagation directions x and y. The starting point for the parametric analysis is based on the following rules: the height of the air gap h_g must be smaller than $\lambda/4$ in order to stop the propagation of all parallel-plate modes. Secondly, the height of metallic pins h_p is supposed to be approximately equal to $\lambda/4$ so that highest surface

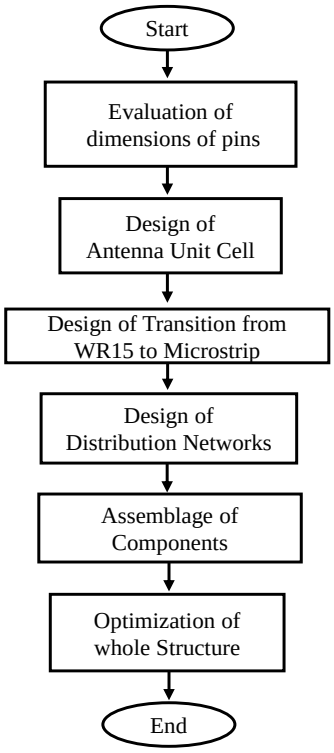

Figure 2.2: The flow chart for design the whole structure in this thesis.

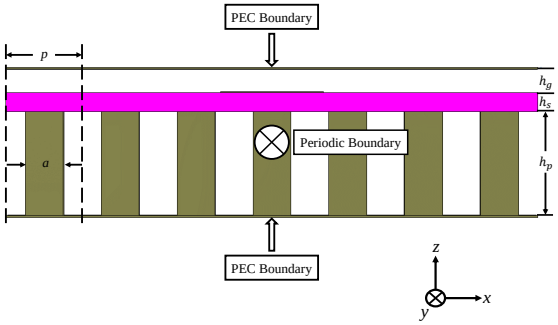

Figure 2.3: Geometrical interpretation of gap waveguide microstrip line. Along the y-axis Periodic Boundary Condition is set up and the structure is simulated in CST Microwave Studio using Eigenmode Solver.

Table 2.1: Geometrical Parameters of the Structure in Figure 2.3

	h_s	h_g	h_p	a	p
Geometrical Parameters	0.2 mm	0.25 mm	1.2 mm	0.4 mm	0.8 mm

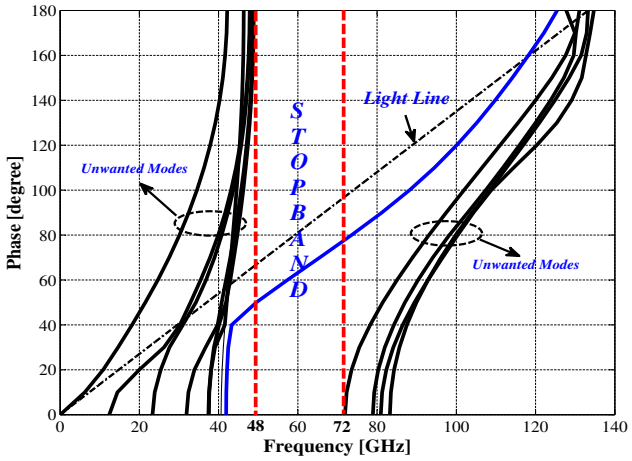

Figure 2.4: Dispersion diagram for the structure in Figure 2.2 and the blue curve crossing over the stopband represents the quasi-TEM mode.

impedance is achieved. The ratio between the width of metallic pins and period a/p has been chosen as 0.5. The considered substrate material is Rogers $RO4003$ with relative permittivity $\varepsilon_r = 3.55$, loss tangent $tan\delta = 0.0027$ (specifications are at 10 GHz according to Rogers material data sheet) and thickness $h_s = 0.2$ mm. It should be emphasized that the loss tangent value of the substrate material Rogers $RO4003$ at 60-GHz frequency band is much higher than that at 10 GHz in reality according to fundamental electromagnetic field theory. Therefore, we have to set up the loss tangent value of Rogers $RO4003$ as 0.01 in CST Microwave Studio, which is almost 4 times higher than the value at 10 GHz. The motivations to select $RO4003$ are that it has lower loss value than traditional PCB substrate $FR4$ and mechanically more rigid than other substrate materials. Correspondingly, the dispersion diagram of the structure is shown in Figure 2.4, which is obtained by utilizing the eigenmode solver in CST Microwave Studio software. The obtained stopband is from 48 to 72 GHz and only one mode propagates within the structure, as shown in Figure 2.4. The corresponding geometrical parameters are listed in Table 2.1.

2.3 Design for Antenna Unit Cell

As mentioned before, a 2×2 element sub-array is firstly designed using periodic boundary condition in order to evaluate the radiation pattern and directivity of whole array antenna. Most importantly, the mutual coupling effect is taken into account in this way so that the periodic boundary conditions in both x and y directions are placed. Figure 2.5 shows exploded perspective view of the 2×2 element sub-array, which briefly consists of radiating slot layer, cavity layer, PCB microstrip layer and

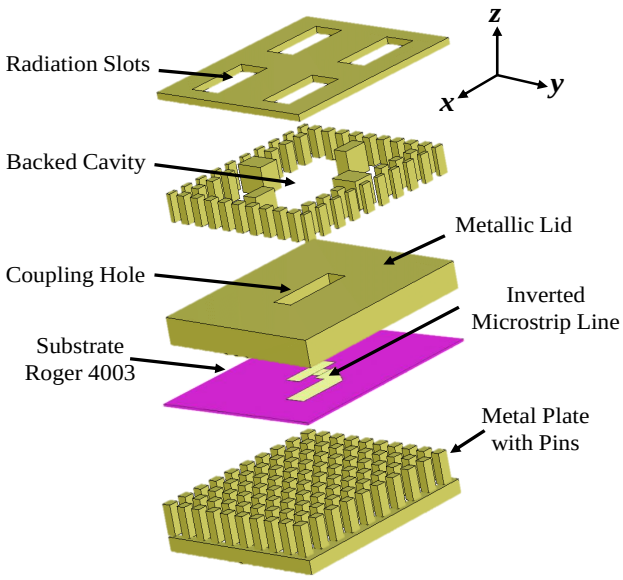

Figure 2.5: Detailed 3-D view of 2 × 2 slots sub-array.

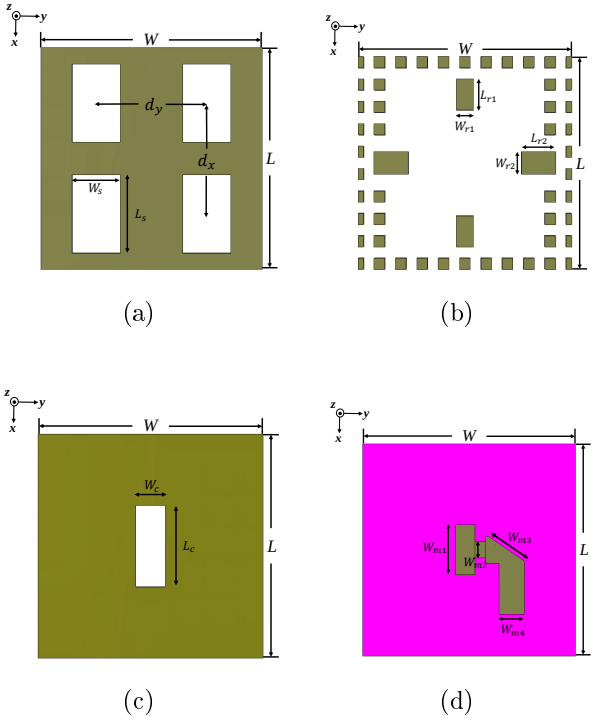

Figure 2.6: Geometrical parameters of a 2 × 2 slots array. (a) Top radiation slots layer. (b) Backed cavity layer. (c) Coupling hole layer. (d) Feed distribution networks layer.

bed of nails. Instead of normal hollow rectangular waveguide cavity, we have utilized groove gap waveguide cavity here because it is convenient to be manufactured. Here the groove gap waveguide cavity in the middle is partitioned into four spaces by two sets of metallic blocks extending in the x and y directions. The PCB microstrip layer feeds all the groove waveguide cavities with identical phase and amplitude by the

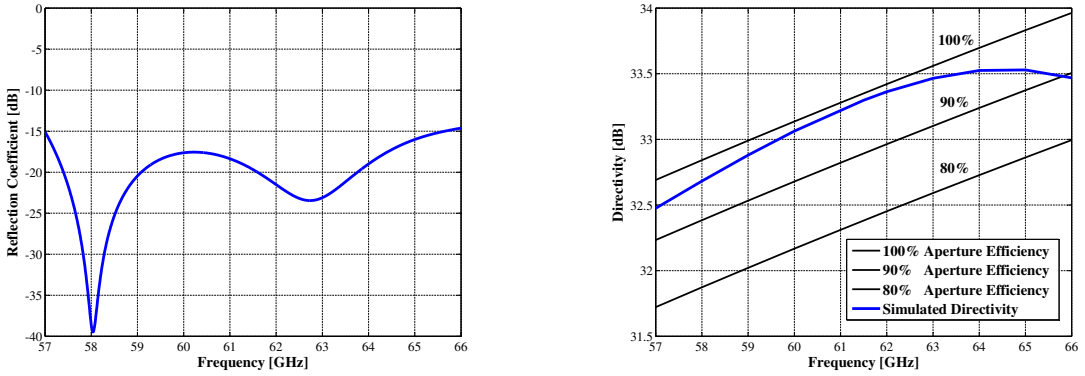

(a) (b)

Figure 2.7: (a) Simulated reflection coefficient S_{11} of 2×2 slots sub-array. (b) Directivity of an array antenna of 16×16 slot aperture dimension in infinite array environment.

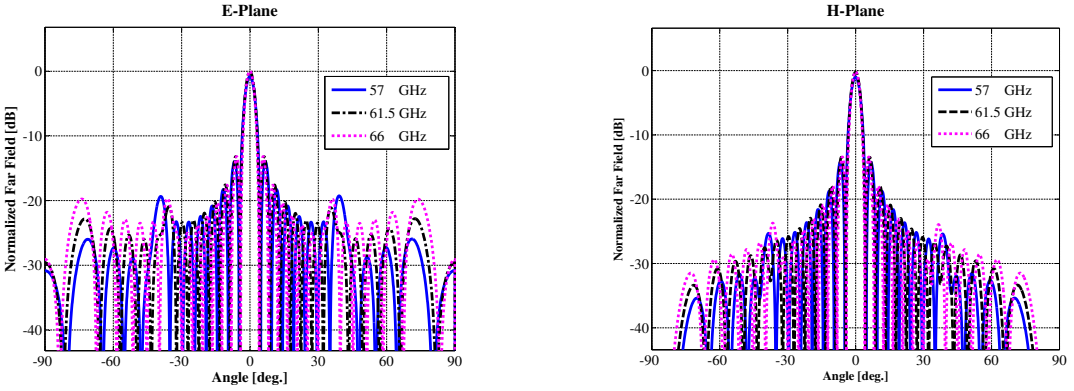

(a) (b)

Figure 2.8: (a) Radiation pattern of 16×16 slot array antenna in E-Plane. (b) Radiation pattern of 16×16 slot array antenna in H-Plane. Both simulation results are obtained by infinite periodic approach on 2×2 slot sub-array.

middle coupling hole.

As is well known, the slots in an antenna aperture ought to be uniformly spaced in both x and y directions with spacing smaller than one wavelength in order to avoid grating lobes in a large broadside array. The highest frequency of the antenna is chosen to be 66 GHz and the corresponding wavelength λ is about 4.5 mm. Therefore,

the slot space d_s in this work we have chosen 4 mm. On the other hand, the value W and L should be integer times of the pins period, namely $W = Mp$ and $L = Np$. Given the above-mentioned considerations, we select $W = L = 10p = 8$ mm. The detailed geometrical demonstration of the antenna sub-array have been shown in Fig. 6. First of all, the slot dimensions W_s and L_s as well as the cavity metallic block dimensions W_{r1}, L_{r1}, W_{r2} and L_{r2} have been well optimized to achieve good radiation pattern. Secondly, W_c, L_c, W_{m1}, W_{m2}, W_{m3} and W_{m4} have been optimized to achieve minimum reflection coefficient. Figure 2.7 (a) shows corresponding reflection coefficient of sub-array and it has 14.5% impedance bandwidth (over 57-65.7 GHz)

Table 2.2: Geometrical Parameters of 2 × 2 Unit Cell the Structure in Figure 2.6

	W	L	d_x	d_y	W_s
Geometrical Parameters	8 mm	8 mm	4 mm	4 mm	1.75 mm
	L_s	W_c	L_c	W_{r1}	L_{r1}
Geometrical Parameters	2.832 mm	1.748 mm	2.742 mm	0.637 mm	1.111 mm

with input reflection coefficient better than -15 dB. Figure 2.7 (b) also illustrates the simulated directivity of 16×16 slot aperture array in infinite array environment. The optimized sub-array achieves that expected design target for whole antenna array. The final dimensional parameters of sub-array are presented in Table 2.2. Here we have utilized the CST Microwave Studio infinite periodic approach along the x and y directions of 8 elements in order to estimate the radiation pattern of the whole structure. Figure 2.8 illustrates the radiation patterns of E- and H-plane of 16×16 slot array antenna according to infinite periodic approach. We have observed that the first side-lobe levels in both E- and H-planes are around -13 dB and the grating lobe levels (GL) in E- and H-planes are respectively below -19 dB and -25 dB.

2.4 Transition from WR-15 to Inverted Microstrip Gap Waveguide

A vertical transition from standard V-band rectangular waveguide to inverted microstrip gap waveguide is presented in this work. Since it is convenient to directly measure antenna array with rectangular waveguide excitation, millimeter wave high gain antennas are usually excited by a standard rectangular waveguide in reality. A standard V-band rectangular waveguide (WR-15) thus works as the input port at the bottom of antenna structure. Obviously, the main challenge here is how to transfer TE_{10} mode in rectangular waveguide to the quasi-TEM mode of inverted microstrip gap waveguide efficiently with simple configureation. Normally there are three types of transitions in microwave technology: inline transitions, aperture coupled patch transitions and vertical transitions. Here we choose the vertical transition.

As sketched in Figure 2.9, this transition is composed of three parts: WR-15

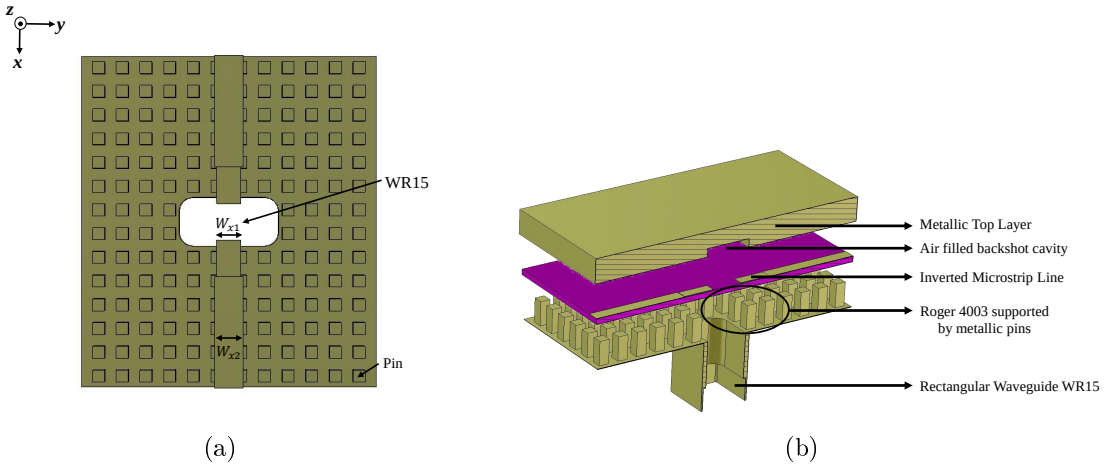

(a) (b)

Figure 2.9: (a) Top view transition geometry. In order to observe the microstrip and waveguide open details the substrate is hidden. (b) Cross-sectional view for complete structure.

feeding waveguide, inverted microstrip gap waveguide and backshort cavity at top metallic layer. The whole structure works as a three-port power divider that can be also utilized for power division. First of all, a PCB is positioned over a bed of pins and

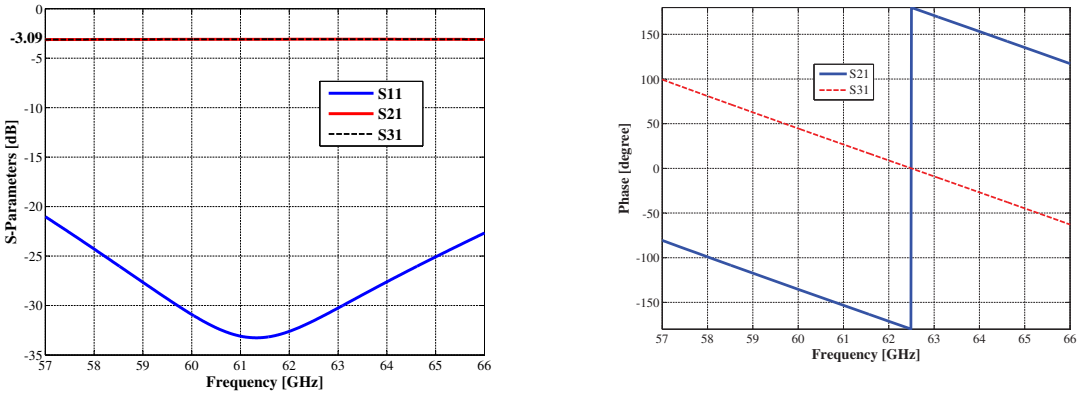

(a) (b)

Figure 2.10: Simulated S-parameter results of designed transition structure. (a) Amplitude. (b) Phase.

it contains tapered section. These tapered-line sections act as an impedance transformer. A parametric sweep of the position and impedance of this tapered section has been carried out in order to achieve optimum return loss within the frequency band of interest. The layout of the transition circuit is shown in Figure 2.9 (a). On the other hand, the whole transition is accomplished by adding a cavity backshort on the top metallic lid, as shown in Figure 2.9 (b). The backshort is positioned opposite

Table 2.3: Geometrical Parameters in Figure 2.9

	W_{x1}	W_{x2}	L_{cbx}	L_{cby}	L_{cbz}
Geometrical Parameters	0.815 mm	0.961 mm	3 mm	1.785 mm	0.375 mm

to the rectangular waveguide opening. Its dimensions are firstly roughly evaluated by impedance transformer and then optimized together with the tapered-line by full wave simulation. The distance between the backshort cavity and the substrate is set as $\lambda_0/4$ ($\lambda_0 = 4.95$ mm) in order to compensate the reactance of two-steps microstrips. Hereby, the backshort cavity together with the tapered microstrip line essentially contributes in field matching as well as impedance matching over 57 - 66 GHz. All significant parameter values are specified on Table 2.3 for this proposed transition power divider. The simulated S-Parameters of the structure is shown in Figure 2.10. The function of simple section is actually equal to a single WR-15 to inverted microstrip gap waveguide transition and a T-junction power divider. In addition, we should notice that the phases of the output ports have 180 degree difference, as shown in Figure 2.10 (b). Please observe that we will compensate this difference in design of distribution networks.

2.5 Design of Feeding Distribution Networks

Compared with groove and ridge gap waveguide structure, the feeding distribution networks based on inverted microstrip gap waveguide has some obvious advantages. First of all, the inverted microstrip gap waveguide has a uniform bed of nails while the other types of gap waveguide prototypes do not. This uniform pins make the fabrication much easier and cheaper. For instance, a uniform pins surface can be sawed with parallel saw blades, whereas nonuniform pin locations and ridges must be milled with a thin milling tool. Secondly, theories and design principles of traditional inverted microstrip technique are very maturate in the past decades so that we can directly utilize them with little modification. For these reasons, the inverted microstrip gap waveguide is attractive in feeding networks for slot antenna arrays at high frequency.

Despite its advantages, the inverted microstrip gap waveguide technology is still a challenge in design of feeding distribution networks for slots array. In [42] a planar horn array fed by inverted microstrip gap waveguide has been already expounded. Since metallic pins surface is able to supply a nearly PMC boundary condition, the distribution networks in [42] has been first designed with an ideal PMC condition instead of metallic pins structure located at the bottom of the substrate. Nevertheless, the corporate-feed networks design in this work differs from that in [42]. Most important reason is that minute quantity of electric- and magnetic fields still exist inside the metallic pins structure in reality while a quasi-TEM mode propagates along

the top microstrip. However, electric- and magnetic fields inside a PMC are both null. Therefore, assuming an ideal PMC condition to replace the metallic pins structure may introduce significant error in design of distribution networks. Until now the inverted microstrip gap waveguide technology has been merely applied for design bandpass filter [43]. Given its complexity an antenna unit cell has been accomplished without distribution networks in [44].

As introduced before, we have already designed a promising antenna unit cell which is fed by inverted microstrip gap waveguide. In this section, a new procedure for design distribution networks based on inverted microstrip gap waveguide structure will be presented. The feeding networks consists of several cascading T-junction power dividers and their impedance matching transformers between each other.

2.5.1 Design of T-junction Power Divider

Essentially a T-junction power divider is a simple three-port network that can be utilized for power division or combining. Thereby, the T-junction is a central component in distribution networks for feeding antenna array. In this work we firstly design a T-

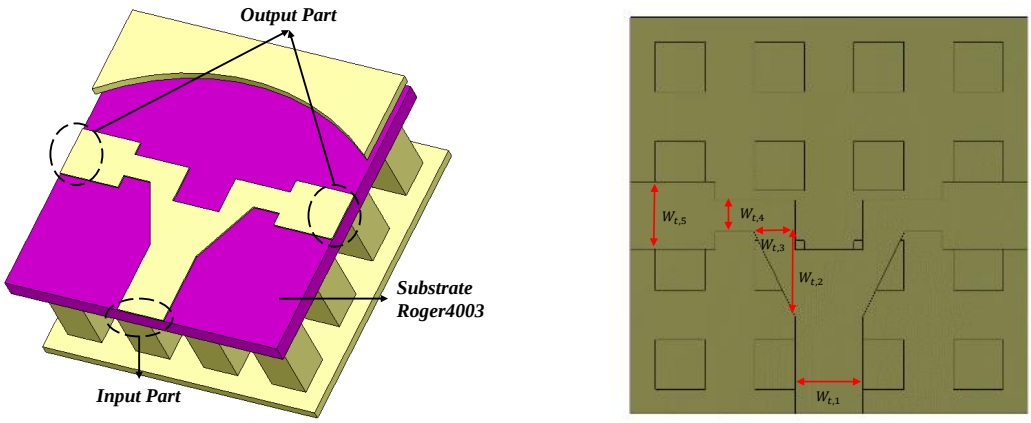

(a) (b)

Figure 2.11: (a) Illustration for single T-junction power divider based on inverted microstrip gap waveguide. (b) Geometrical description for single T-junction and the substrate is hidden in order to observe the microstrip and bottom bed of nails.

junction power divider with metallic pins in CST Microwave Studio shown in Figure 2.11 (a). In order to obtain correct transition performance an optimized numerical port [45] has been utilized during the entire design procedure. The T-junction then has been optimized with the dimensions of width of microstrips $W_{t,1}$, $W_{t,2}$, $W_{t,3}$, $W_{t,4}$ and $W_{t,5}$ and the final optimized geometrical parameters are listed in Table 2.4. Fig. 12 shows S-parameters, where the reflection coefficient S_{11} is below -30 dB from 57 to 66 GHz. The S_{21} and S_{31} are identical to -3.1 dB. Besides the lost energy in sub-

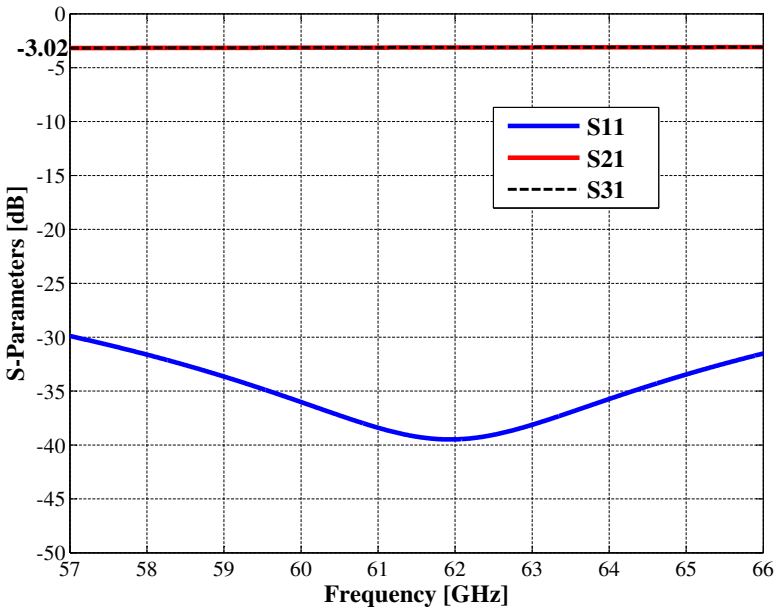

Figure 2.12: The simulated S-parameters of single T-junction.

Table 2.4: Geometrical Parameters in Figure 2.11

	$W_{t,1}$	$W_{t,2}$	$W_{t,3}$	$W_{t,4}$	$W_{t,5}$
Geometrical Parameters	1.045 mm	1.324 mm	0.306 mm	0.298 mm	1.100 mm

strate $RO4003$, the rest of electromagnetic energy are identically split to output port 2 and port 3. The simulated result also indicates that T-junction power divider has promising abilities of power division and isolation for two output ports. The input and output port impedances are calculated by CST and it is convenient to utilize them for impedance transformer design in next subsection.

2.5.2 Design of Impedance Transformer

Impedance matching is a practical topic in microwave circuits. This fundamental idea is that an impedance matching network placed between a load impedance and a transmission line. The reflection effect will be eliminated on the distribution networks to the matching networks. The basic principle of impedance matching is shown in Fig. 13 (a) and its implementation in this work is shown in Fig. 13 (b) as well. In this work we apply classical second order binomial impedance transformer for impedance matching. All characteristic impedances and load impedances has been obtained from optimized numerical ports introduced in [45]. Here we should notice

(a)

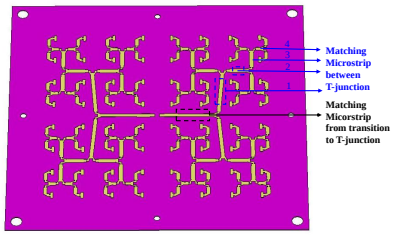

(b)

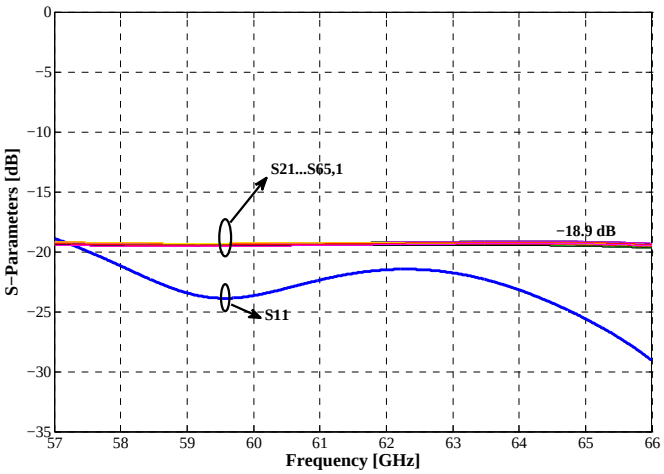

(c)

Figure 2.13: (a) Illustration for a network matching an arbitrary load impedance to a transmission line. (b) Realized whole feeding networks and its matching parts in this work. (c) Simulated S-Parameters in CST Microwave Studio.

that part 1 of matching microstrip has been designed as shape of parallelogram in order to remove its mutual coupling effect to the nearest coupling holes. In addition, the input port in CST is set up at the bottom of WR-15 and the output ports are built at the output microstrip of last stage T-junction power divider. Finally, the whole distribution network is optimized by genetic algorithm.

The final designed structure of the feeding distribution networks is shown in Fig. 13 (b). The complete corporate-feed network consists of two 32-way power dividers connected to the transition of WR-15 at the center. As described in section IV, the transition power divider from WR-15 to inverted microstrip gap waveguide has 180 degree phase difference. Thereby, the whole feeding network is mirrored in order to compensate the phase difference. Fig. 13 (c) shows the corresponding S-parameters of the whole distribution networks. The reflection coefficient S_{11} is almost below -20 dB over 57 - 66 GHz.

2.6 Comparison between Simulated and experimental results

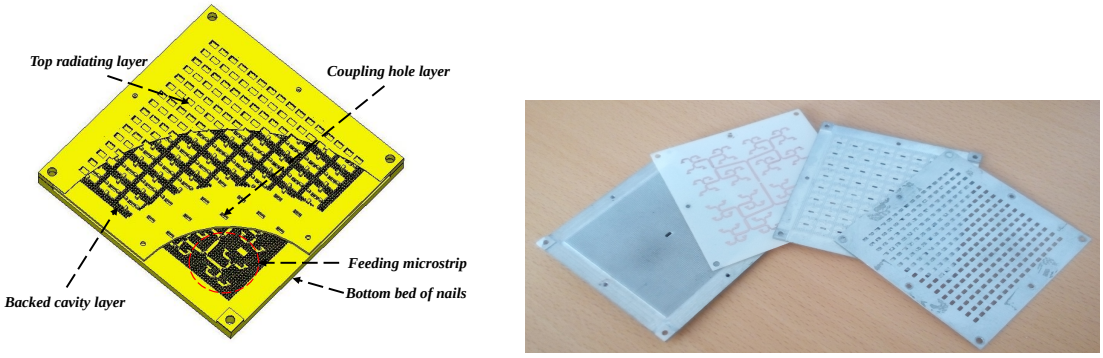

(a) (b)

Figure 2.14: (a) Numerical model in CST Microswave studio of proposed array antenna. In order to observe the microstrip and waveguide open details the substrate is hidden. (b) Photogragh of proposed 16×16 array antenna fabricated by EDM technology.

The numerical model and final manufactured prototype of the 16 ×16 slot array antenna discussed in this paper is shown in Fig. 14. The metallic parts of the array antenna is fabricated by Electrical Discharging Machining (EDM) Technology. In this manufacture technology, the designed prototype is etched by recurring electric discharges between the workpiece and electrodes. The final designed array aperture dimension is 64 × 64 mm^2 (8 mm×8 mm× 64 elements).

The simulated and measured input reflection coefficients of the proposed antenna

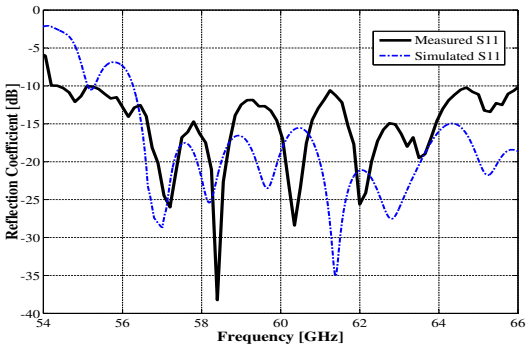

Figure 2.15: Comparison of simulated and measured reflection coefficient of the proposed 16 × 16 slot array antenna.

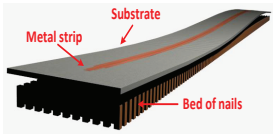

Figure 2.16: Sketch of inverted microstrip gap waveguide with a bent substrate.

are shown in Fig. 15. The measured S_{11} is a bit higher than the simulation. However, it is still below -10 dB from 54.5 GHz to 66 GHz (19.2% impedance bandwidth). There are some differences between the simulated and measured results. As above discussed in section II, the dispersion diagram of whole structure is affected by dimensions of metallic pins, the thickness of substrate and the height of air gap. Therefore, any manufacture tolerances of bed of nails and the height change of air gap will cause shift of parallel stopband. As reported in [46], there is always a frequency shift in reflection coefficient which drifts towards to lower or higher frequency. A consequence of this is that the PCB may not remain rigidly supported over the bed of pins, and there are some points in which the pins do not have a good contact with the substrate (see sketch presented in Fig. 16). Furthermore, these untouched gap between substrate and pins automatically creates capacitance effect. This small shunt capacitor affects the dispersion diagram of inverted microstrip gap waveguide.

The radiation pattern of proposed antenna is measured in an anechoic chamber. The simulated and measured normalized radiation patterns in the E- and H-plane at four different frequencies 57, 60, 61, 66 GHz are shown in Fig. 17 and Fig. 18. The measured Co-polarization radiation patterns show a very good agreement with the simulated results. The simulated and measured radiation patterns are symmetrical, and the first side-lobe levels in both E- and H-planes are around -13 dB. The measured grating lobes of the fabricated array in both E- and H-planes are below -20 dB

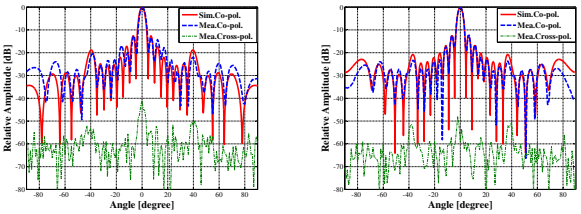

(a) (b)

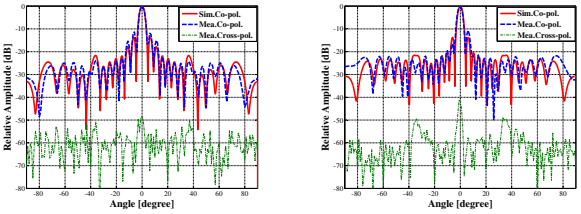

(c) (d)

Figure 2.17: Measured and simulated radiation pattern of proposed array antenna on E-plane. (a) 57 GHz. (b) 60 GHz. (c) 61 GHz. (d) 66 GHz.

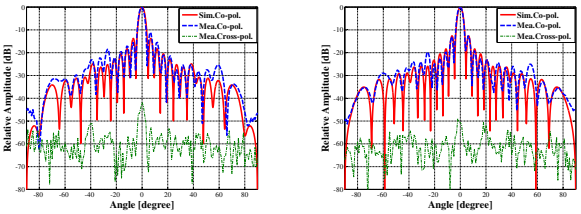

(a) (b)

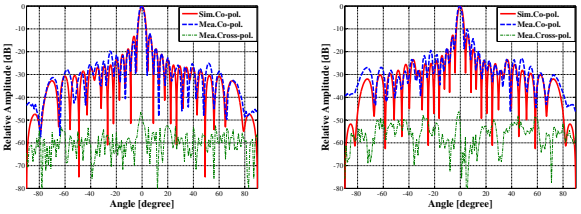

(c) (d)

Figure 2.18: Measured and simulated radiation pattern of proposed array antenna on H-plane. (a) 57 GHz. (b) 60 GHz. (c) 61 GHz. (d) 66 GHz.

over the desired frequency band. The cross-polarization values are below -40 dB at all frequencies.

The simulated directivity and gain of proposed antenna are shown in Fig. 19. The red solid line, which stand for simulated directivity, is above 80% aperture efficiency ($64\times64\ mm^2$). The pink dash line in Fig. 19 indicates the simulated gain after setting up the modified loss tangent of substrate. This method help us accurately predict the real gain after manufacturing. The blue dash-dot line in Fig. 19 shows the measured

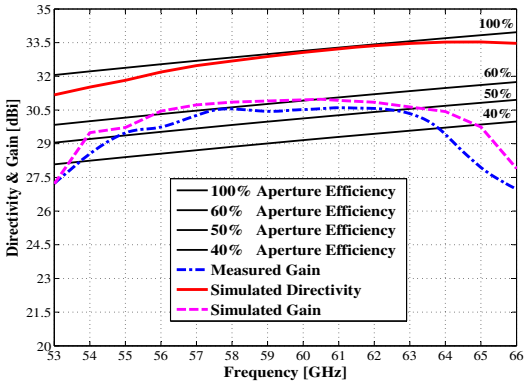

Figure 2.19: Measured gain and simulated directivity of present 16 × 16 slot array antenna.

gain, illustrating above 40% aperture efficiency over the frequency band 54-64 GHz. What we should notice in Fig. 19 is that the measured gain drops very rapidly at the start of 64 GHz, yet our design target is 57-66 GHz. The probable explanation for reducing of antenna gain of proposed array antenna is that the true loss tangent of substrate is actually unknown in reality. The value of tangent loss is probably even higher than 0.01 at higher frequency band. The other possible reason for the gain reduction is that the antenna is made of steel. The top radiating layer is too thin to be deformed by the force. The analogues phenomenons also appear in [47] and [48]. Compared with the designs in [47] and [48], our work exhibits wide impedance bandwidth, higher aperture efficiency and low cost on fabrication. However, because of the ohmic loss in dielectrics of feed distribution networks, the realized gain of our work is lower than those reported in [49], [50] and [51]. Thereby, there are still some work to do for the further improvements. As illustrated in Fig. 16, the untouched gap between pins and substrate is most important issue because it produces negative effect on wave propagation of the structure. How to solve this problem is an important issue for this technology.

2.7 Conclusion

A high gain and wide bandwidth slot array antenna based on inverted microstrip gap waveguide at 60-GHz has been presented in this work. The proposed antenna consists of four unconnected layers without any electric contact between them. The designed prototype is manufactured by EDM technology. In this paper, we firstly used we used a new corporate feed network based on the inverted microstrip gap waveguide technology. A transition power divider between WR-15 and inverted microstrip gap waveguide have been designed in order to provide a simple excitation of the antenna. The simulated and measured results of the whole antenna structure shows very good agreements in radiation patterns in both E- and H-plane. The measured realized gain is higher than 29 dBi over the entire operation bandwidth from 54.5 to 64 GHz, corresponding to efficiency larger than 45%. This work shows that the inverted microstrip gap waveguide technology is an excellent candidate for array antennas in millimeter wave communication.

Chapter 3

Slot Array Antenna based on Groove Gap Waveguide in the W-Band

The newly introduced gap waveguide technology offers non-contact waveguide configurations so that the good electrical contact between different metallic layers can be avoided. Thereby, the gap waveguide structures are relatively simple to manufacture, especially at millimeter and sub-millimeter wave frequencies. This work systematically presents a high-efficiency corporate-fed slot array antenna based on groove gap waveguide in the millimeter waves. A cavity-backed slot sub-array is firstly designed in a groove gap waveguide cavity. The cavity is fed through a coupling hole from groove gap waveguide distribution network at the bottom layer. The sub-array is numerically optimized in an infinite array environment. Low side lobes are obtained in the both E- and H-planes by diagonal placement of the radiation slot rotating by 45 degrees. Furthermore, the radiation narrow slot pair is adopted so that the good cross polarization is achieved. The fabricated antenna depicts more than 25% bandwidth with input reflection coefficient better than -8 dB and the aperture efficiency higher than 60% with around 25 dBi realized gain between 70 and 90 GHz. The measured cross polarization level is below -27 dB, which satisfies the ETSI standard.

3.1 Introduction

Recently, the saturation of spectrum at microwave frequencies causes the consideration of higher frequency bands. Especially, the millimeter wave range between 30 GHz and 300 GHz has been paid lots of attentions. Furthermore, the usage of the millimeter wave frequencies has the advantage of allowing for larger bandwidths, and thereby, achieving higher data transfer rates. In such frequency ranges, traditional hollow waveguide and microstrip lines have met up with difficulties to design antennas and passive components.Indeed, hollow waveguide are normally manufactured in two parts and then joined together. In microwave frequency band, it is still convenient to

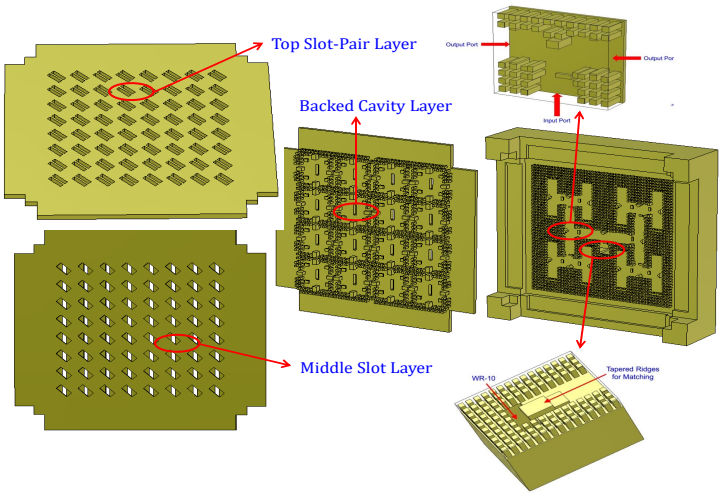

Figure 3.1: Configuration of the proposed corporate-feed slot array antenna based on groove gap waveguide.

fabricate hollow waveguide because its geometrical dimensions are large. However, its fabrication becomes a big problem because its dimensions are very small in millimeter waves. Moreover, it suffers from problems of irregular rectangular shape and poor electrical contacts. Diffusion bonding and vacuum welding are probably two manufacture technologies for hollow waveguide in millimeter waves. Nevertheless, its fabrication cost is relatively high. On the other hand, microstrip lines or covered microstrip lines are able to integrate the active components, but still present high dielectric losses in millimeter waves. Thereby, new technologies in millimeter waves are still demanded.

Substrate integrated waveguide (SIW) is an appropriate candidate in millimeter waves. Nevertheless, it exhibits undesired dielectric losses in the substrate at increasing frequencies. As is well known, the loss tangent value of substrate increases versus the frequency. Thereby, the dielectric loss in SIW is unacceptable above 60 GHz so that the antenna efficiency is affected. In such a situation, there is still need to find new technological solutions for waveguides that have low losses and are cheap to manufacture. The recently introduced gap waveguide technology constitutes a new type of guiding structure that shows lot of potential to overcome the issues of conventional technologies, and become a suitable approach at millimeter wave frequencies. First of all, the gap waveguide shows low loss compared with microstrip, covered microstrip and SIW. Secondly, unlike the conventional manufacture of hollow waveguide, the gap waveguide structure is very flexible to be manufacture. Most importantly, the electrical contact between the building blocks is not needed in this new guiding structure so that expensive fabrication technologies, such as vacuum welding and diffusion

bonding, can be avoided in millimeter waves. Until now four different variety of gap technology, ridge gap waveguide, groove gap waveguide, microstrip-gap waveguide, and inverted microstrip-ridge gap waveguide have been already investigated. They are able to achieve characteristics of high-gain and high-efficiency because of low loss property.

In this work, we Initially introduce a 45^o linearly polarized corporate-feed groove gap waveguide slot array antenna covering 71.5 to 90 GHz. As depicted in Figure 3.1, the whole slot array antenna consists of the distribution feeding networks, the backed cavity layer, the middle slot layer and the top radiation slot layer. The feeding part is composed of equally-split H-plane T-junctions and a vertical transition from WR-10 standard hollow waveguide from its back. In order to satisfy the radiation pattern of ETSI standard, the radiation slots usually have been 45^o rotated. Given the rising of the cross polarization level caused by 45^o degree rotation, a narrow-slot pair configuration on the top is designed to suppress the cross-polarization. The proposed antenna has been fabricated by computerized numerical control (CNC) milling machine. The measured reflection coefficient and far-field radiation patterns are discussed in the end.

3.2 Design of Sub-array

The pin dimensions of bed of nails at both distribution networks and backed cavities should be chosen correctly to achieve a parallel plate stopband which covers as much as the operating frequency. As depicted in Figure 3.2(a), the design unit cell of proposed groove gap waveguide is built with PEC, periodic and PEC boundary conditions in x-, y- and z-axis in CST Microwave Studio, respectively. Correspondingly, the dispersion diagram of the structure is shown in Figure 3.2(b), which is obtained

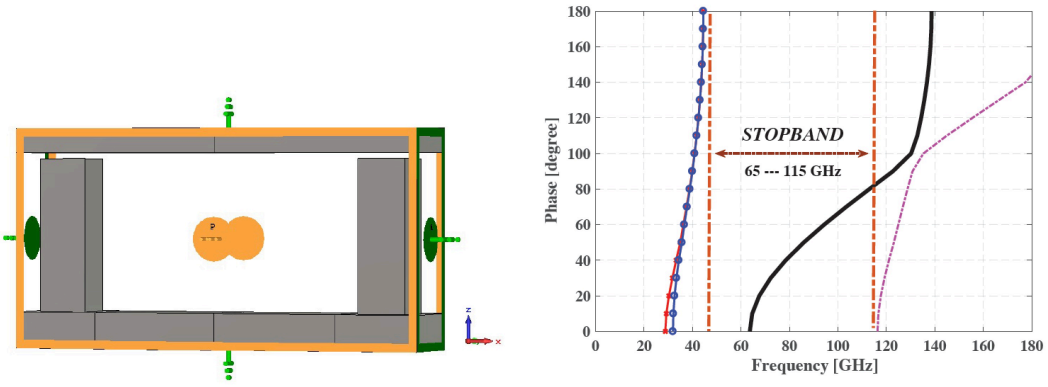

(a) (b)

Figure 3.2: (a) A groove gap waveguide unit cell for determination of dispersion diagram. (b) The corresponding dispersion diagram.

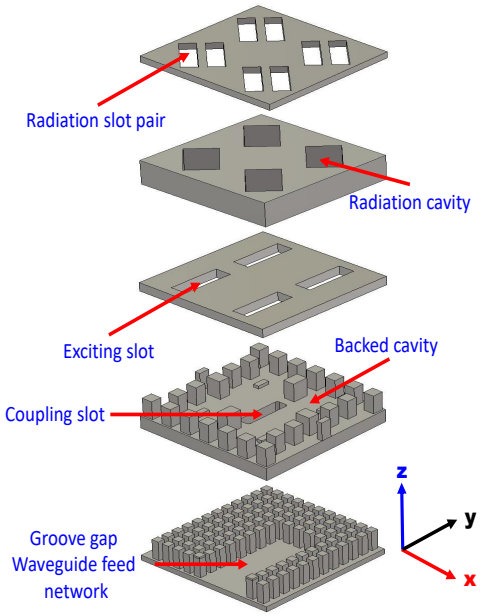

Figure 3.3: Model for the analysis of the 2×2-element sub-array.

by utilizing the eigenmode solver in CST Microwave Studio. The obtained stopband is from 65 to 115 GHz. The proposed 2×2 sub-array is illustrated in Figure 3.3. The sub-array consists of four layers - the top pair radiation layer, the middle slot layer, the backed cavity layer and the bottom distribution feed networks layer. An air-filled

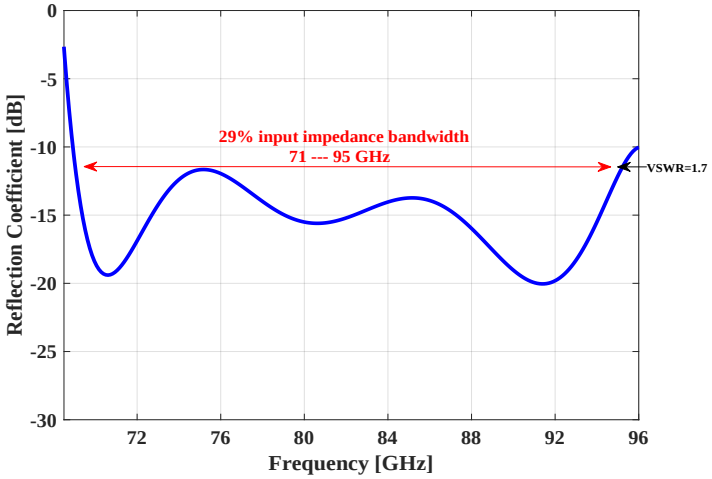

Figure 3.4: The reflection coefficient of the sub-array.

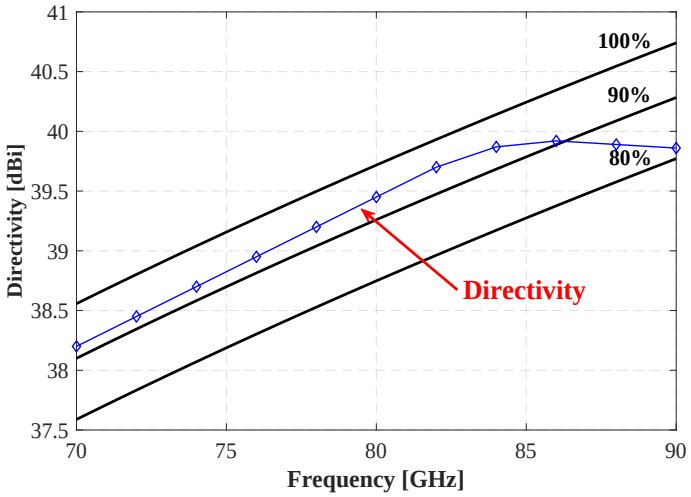

Figure 3.5: The simulated directivity of the 32×32 slot array according to the periodic boundary condition.

cavity formed by pins, feeds four radiating slots with spacing smaller than 3.1 mm, which is equal to one wavelength on the top layer. A groove gap waveguide excites the cavity via a coupling slot on the bottom layer. There is a small gap between each layers and thereby no electrical contact between the different layers. This is a manufacturing advantage of this technology. The designed sub-array has 6×6 mm^2 dimensions. The sub-array is optimized in the infinite array environment by using CST Microwave Studio where the mutual coupling between sub-arrays are automatically included. The simulated reflection coefficient of the sub-array is illustrated in Figure 3.4. The sub-array bandwidth is 29% (71 — 95 GHz) with the VSWR better than 1.7. The directivity versus frequency of an array with the same aperture size

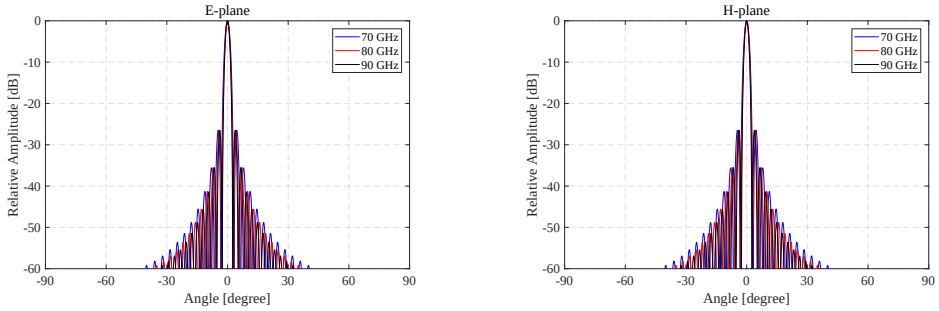

(a) (b)

Figure 3.6: Normalized radiation patterns of an array with 32 × 32 slot aperture dimension in (a). E-plane and (b). H-plane. Infinite array approach.

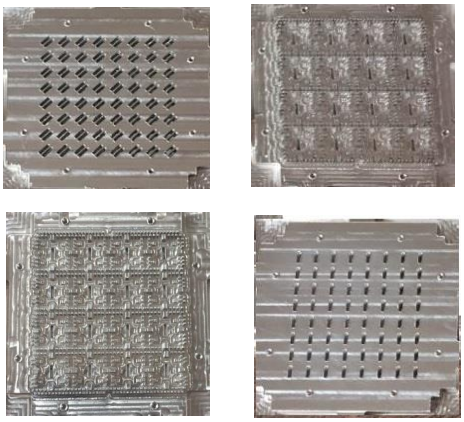

Figure 3.7: Picture of manufactured antenna in this work.

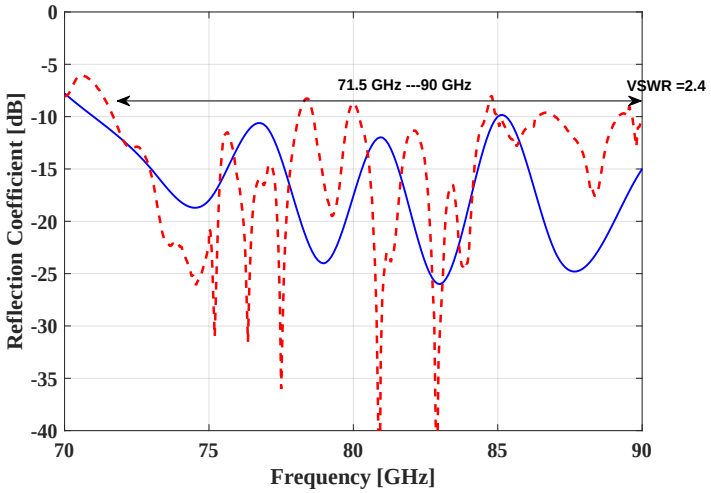

Figure 3.8: The simulated and the measured reflection coefficients of proposed antenna. The blue curve indicates the simulated reflection coefficient, and the red line depicts the measured one.

is shown in Figure 3.5. The blue line in the graph shows the maximum available directivity between 100% and 80% aperture efficiency, which clearly shows that the designed sub-array has high aperture efficiency. In Figure 3.6, the E- and H-plane far field patterns of an array with 32×32 slots over its aperture are illustrated for different frequencies.

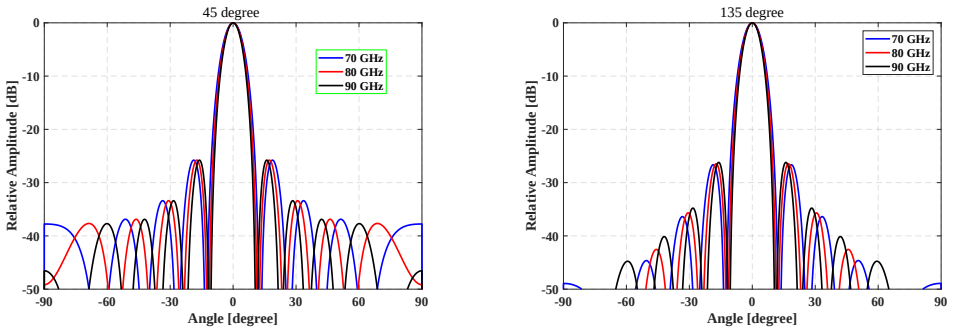

Figure 3.9: The simulated far-field radiation patterns of proposed antenna. (a) E-plane and (b) H-plane.

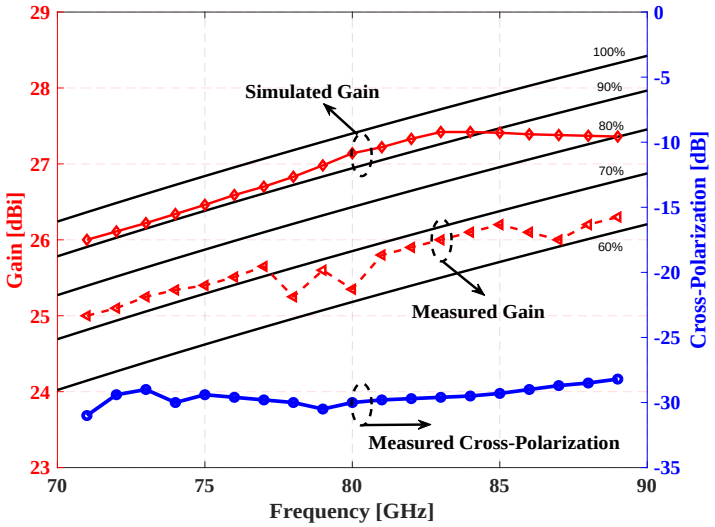

Figure 3.10: The simulated and measured gains of the proposed array antenna. The measured one shows the antenna efficiency is higher than 60%. The measured cross-polarization is better than -27 dB, which fulfills the ETSI standard.

3.3 Simulation and Measurement for the 8×8 Slot Array

The fabricated 8×8 slot array antenna is illustrated in Figure 3.7. The prototype is manufactured by Computerized Numerical Control (CNC) technology. The fabricated machine is Fanuc α D14B15 with fabrication tolerance 2.5 μm, and this is good enough to fabricate our array antenna. The dimensions of effective aperture are 24×24 mm^2 and it was fabricated by Aluminium (with electric conductivity 3.6 ×

10^7 S/m). The entire structure is simulated in CST Microwave Studio. The simulated reflection coefficient of complete antenna is below -10 dB from 70 to 90 GHz, as shown in Figure 3.8. However, the measured reflection coefficient is a bit higher than simulated one because of the tolerances of manufacturing and assembling tolerances. Still, it covers 71.5 to 90 GHz with the VSWR better than 2.4. The simulated far-field radiation patterns of proposed antenna at 70, 80 and 90 GHz in both E- and H-planes are depicted in Figure 3.9. Low sidelobe characteristics are obtained over the bandwidth investigated here. No grating lobe is observed. The simulated first sidelobe levels are less than -26 dB. The measured frequency characteristics of the gain and the cross polarization are shown in Figure 3.10. The gain and the cross polarization are measured by V- and W-band far-field measurement systems for 70—75 GHz and 75—90 GHz, respectively. In the 71—89 GHz band, the gain variation is 25—26.2 dBi. The bandwidth for a gain of more than 25 dBi and the antenna efficiency of more than 60% is greatly improved. The cross polarization is suppressed below -27 dB over the full bandwidth.

3.4 Conclusion

In this work, we present a 45 degree 8×8 cavity-backed slot array antenna based on groove gap waveguide for high-gain 80 GHz. The proposed antenna consists of four layers, i.e. 45 degree radiation slot layer, middle coupling slot layer, backed cavity layer and feeding network layers without need of electrical contact between layers. This presents manufacturing advantages in particular at millimeter wave. The array antenna can be directly connected with standard WR-10 interface. The measured gain is higher than 25 dBi from 71 to 90 GHz, correspondingly the antenna efficiency larger than 60%.

Chapter 4

A Single-Layered Corporate-Feed Slot Array based on Ridge Gap Waveguide in the V-Band

This paper presents an 8×8-element slot array antenna with single-layered corporate-feed based on the ridge gap waveguide technology in the 60-GHz band. As is well-known, a corporate-feed slot array antenna usually has backed cavities to increase the bandwidth and provide a space for its distribution network, and therefore three layers in total: one layer for radiating slots and two layers for feed network with one layer of back cavities and one of power dividers. The antenna in this work is designed by utilizing only two separate metallic layers – a corporate-feed network layer and a radiating slot layer. Compared with the conventional three-layered slot array antennas, the proposed antenna avoids the utilization of the backed cavity layer so that its complexity and manufacture cost decrease. In order to solve the problem of the narrow bandwidth caused by taking away the backed cavities we utilize double-ridged radiating slots instead of the conventional rectangular ones. A compact transition power divider from standard waveguide WR-15 to the ridge gap waveguide is introduced to excite the proposed array antenna. The 8×8-element slot array antenna has been fabricated by computerized numerical control machining technique. The measured results demonstrate that the -10 dB reflection coefficient has around 17% bandwidth covering 56.5 – 67 GHz frequency range, and the measured gain is better than 26 dBi with more than 70% antenna efficiency over 58 – 66 GHz.

4.1 Introduction

Recently, the current saturation of spectrum at microwave frequencies causes new attention to the millimeter waves (mmWs). Hence, the unlicensed 60-GHz band (from 57 to 66 GHz) has a very strong potential for high data rates wireless com-

munications. However, the communication distance at 60-GHz is strongly affected by atmospheric absorption. Thereby, an antenna with high-gain and wideband is theoretically required for such kind of point-to-point wireless systems. The reflector antenna is normally a conventional choice. Nevertheless, thin planar slot array antennas are more desirable in the 60-GHz frequency band due to its high efficiency and thin profile. Recent popular technology to mmWs is the substrate integrated waveguide (SIW). Nevertheless, its dielectric loss becomes problematically significant if it is applied for designing large high-gain array antennas in the 60-GHz band.

The gap waveguide is a new technology recently introduced. Theoretically, this new waveguide consists of two parallel plates, a top plate of perfect electric conductor (PEC) and a bottom plate of perfect magnetic conductor (PMC). If the air gap between the parallel plates is smaller than quarter-wavelength, there is no propagating wave between the plates. However, if a wave guiding structure, such as a microstrip or ridge, is added between the PEC-PMC plates, a quasi-TEM mode is able to propagate along the guiding structure. Given the non-existence of PMC in nature, the metallic pins surface is applied to realize Artificial Magnetic Conductor (AMC). This novel gap waveguide has advantages compared to the microstrip line and the hollow waveguide. First of all, the gap waveguide can keep a planar profile as well as being low loss since the waves propagate in the air gap. Secondly, this technology can avoid the requirement of good metallic contacts between the parallel metallic plates because the metallic pins surface can create a high impedance to avoid the wave leakage. In addition, the gap waveguide makes fabrication process easy and cheap by molding or die-sink electrical discharge machining (EDM) technique. Furthermore, the AMC of gap waveguide technology can be utilized to package active components and low-cost bandpass filters.

So far, there are four different realizations of gap waveguide technology — groove, ridge, inverted microstrip and microstrip-ridge gap waveguides. two high-gain high-efficiency slot array antennas in V-band on ridge gap waveguide (RGW) have been reported. In previous chapter, a classic double-layer full corporate-feed slot array antenna based on inverted microstrip gap waveguide has been introduced. In order to achieve wideband and provide enough space for the distribution networks, this array antenna has backed cavities where four slots are fed by one cavity. Therefore, such a type of antennas consist of three layers — distribution feed networks, backed cavities and radiation slots. Some typical examples are shown in Figure 4.1. Unfortunately, it is inevitable to increase the manufacture cost and design complexity for designing those corporate-feed antennas. On the other hand, instead of using the corporate-feed network, a series-feed network is commonly applied for a single-layered fed slot array because its structure is simple. Nevertheless, its congenital disadvantage is also obvious. The bandwidth is usually limited to several percentage because of the long line effect. Thereafter, it is much preferred to have a slot array with single-layered corporate-feed network.

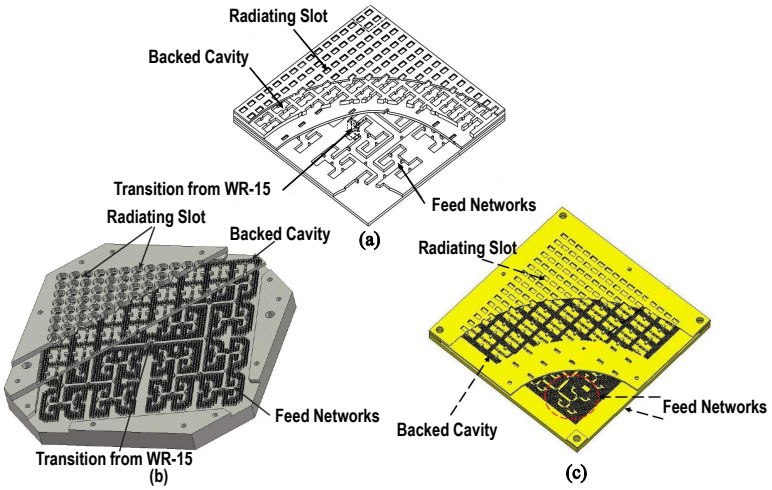

Figure 4.1: (a) depicts a cavity-backed slot array antenna fed by hollow waveguide. (b) shows a cavity-backed slot array antenna fed by ridge gap waveguide and a similar antenna fed by inverted microstrip gap waveguide stated is illustrated in (c). These three full corporate-feed antennas consist of three layers — distribution feed networks, backed cavity and radiation slots and their operating frequency all in the 60-GHz band.

In this chapter, we initially introduce a new slot array antenna with single-layered corporate-feed network in the 60-GHz band. This novel antenna avoids utilization of the backed-cavities by a new layout of the corporate-feed distribution network in RGW and meanwhile achieves expected radiation pattern. The shape of the radiation slots is a modified double-ridge waveguide, which has a wider bandwidth than that of rectangular slots with a single-layered corporate-feed network.

4.2 Geometrical dimensions of RGW for stopband, transition and mutual coupling

Based on the fundamental theory, a gap waveguide supplies a stopband over a specific frequency range between the two parallel-plates. Since our target is to cover the whole unlicensed 60-GHz frequency band (57-66 GHz), the dimensions of the RGW should be properly chosen to cover as much of the 60-GHz frequency band as possible. A simple geometrical schematic diagram of the RGW is depicted in Figure 4.2. A center frequency of $f_0 = 62$ GHz is assumed in this work. Then the height of the pins should be typically selected as $\lambda_0/4$, which is equal to 1.2 mm. Nevertheless, for the easier manufacture shorter pins have been chosen in this work. Furthermore, for achieving good radiation patterns the spacing between any two slots is selected as 4.2 mm, which is equal to $0.87\lambda_0$. Having considered the layout of the distribution

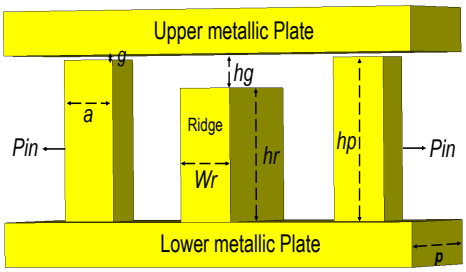

Figure 4.2: The geometrical dimensions of the ridge gap waveguide for the array antenna in this work.

Table 4.1: Geometrical Parameters in Figure 4.2

	W_r	h_r	g	h_g	h_p	a	p
Geometrical Parameters	0.55 mm	0.75 mm	0.03 mm	0.2 mm	0.92 mm	0.4 mm	1.05 mm

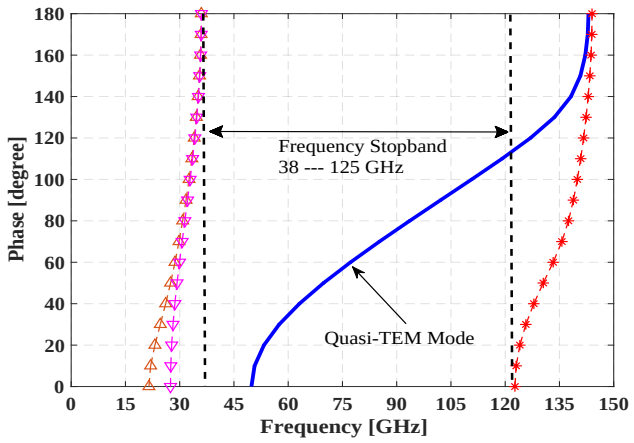

Figure 4.3: Corresponding dispersion diagram of the ridge gap waveguide depicted in Figure 4.2. The blue solid line stands for the Quasi-TEM mode.

network, four rows of metallic pins are required for the dimension of 4.2 mm and the corresponding periodicity of metallic pins is 1.05 mm. On the other hand, the width of square metallic pins is chosen as 0.4 mm. Thereby, the spacing between two arbitrary pins is 0.65 mm, which is equal to the difference of two mentioned variables. The dispersion diagram of the ridge gap waveguide is depicted in Figure 4.3. The stopband is from 38 to 125 GHz, which covers the whole V-band.

In corporate-feed array antennas, the space for the layout of ridge lines is usually very limited so that the backed cavities is applied to provide more space for the distribution feed network. Therefore, it is a big challenge to lay out feed networks

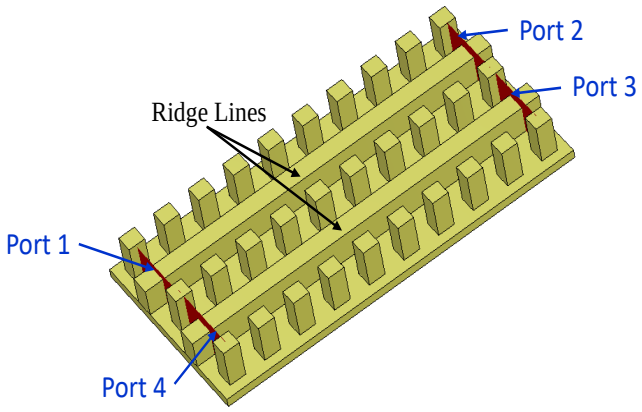

Figure 4.4: Top view of two parallel ridge lines with one row of pins in between. Upper flat metallic plate is hidden to illustrate the bottom plate.

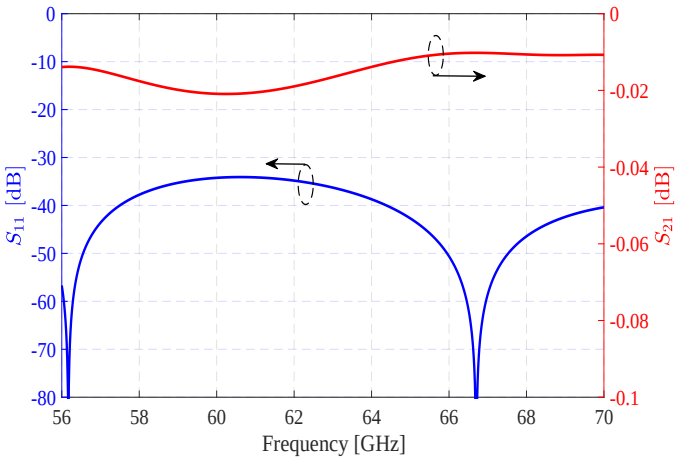

Figure 4.5: Simulated reflection coefficient and the transmission coefficient of the two parallel RGWs in Figure 4.4.

without backed cavities in this work. Before designing the whole array antenna, the coupling between two ridge lines with only one row of pins should be tested. Figure 4.4 illustrates a simple model to examine the performance. The length of the whole structure is 10.5 mm. While the height of the metallic pins h_p is already fixed, we have to search for the optimal dimensions of air gap height g, the width W_r and the height h_r of the ridge in order to minimize the reflection coefficients and the coupling S_{31} between two ridge lines with only one row of pins. As illustrated in Figure 4.5, the reflection coefficient of the straight ridge line is below -33 dB from

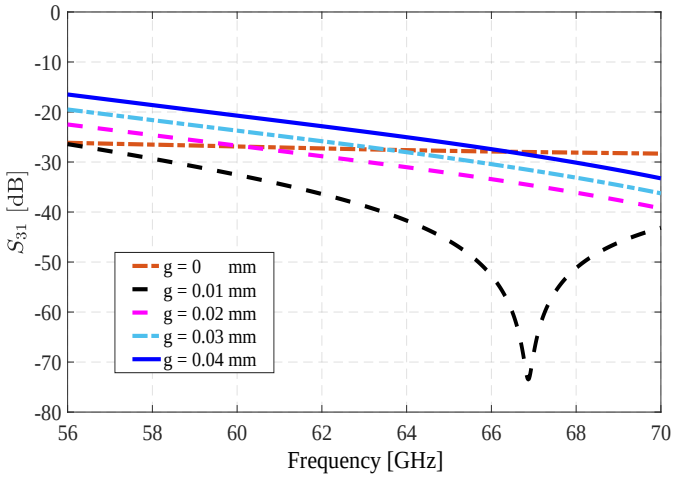

Figure 4.6: Mutual coupling investigation on one row pins between two straight ridge lines defined in Figure 4.2. Parameter sweep for g is carried out in CST Microwave Studio.

56 to 70 GHz. This outcome is acceptable for the array antenna design in this work. The parameter sweep method is also utilized for g stated in Figure 4.2 in this part in order to minimize the mutual coupling between the two ridge lines. As is shown in Figure 4.6, the mutual coupling is lower than -20 dB when the air gap between the metallic pins and upper metallic plate g is smaller than 0.03 mm. This value is acceptable for designing distribution feed network based on RGW only with one row of pins. Having considered the requirement of non-electrical contact, we have selected 0.03 mm in this work and it presents that the feed network has very low leakage and mutual coupling between two neighbor ridge lines with one row of pins in the 60-GHz band.

4.3 Design of Antenna Unit Cell

As depicted in Figure 4.7, the antenna unit cell consists of a radiating slot and a ridge feeding line. This element is under periodic boundary condition defined in CST Microwave Studio. The slot in this work is designed as an '8' shape, which is actually a double ridge slot with circularly curved corners and smoothly profiled ridges. The double ridges will lower the cutoff frequency of the dominant mode and will raise the cutoff frequency of the next higher order modes in the slot. Therefore, it increases the bandwidth of the array antenna compared with that by using a normal rectangular slots. To excite the electromagnetic wave in the slot, the magnetic field created by the ridge line of feed layer should rotate along the vertical direction of the double ridged slot. Then electromagnetic wave can radiate with same phase and polarization from

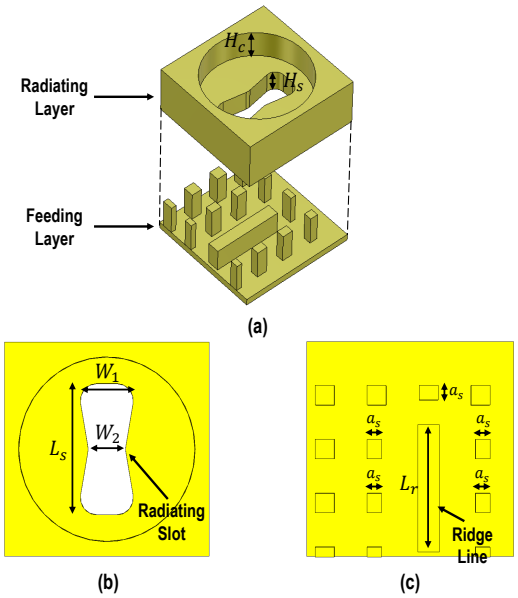

Figure 4.7: Proposed antenna unit cell: (a) Exploded view. (b) Radiating layer. (c) Feeding layer.

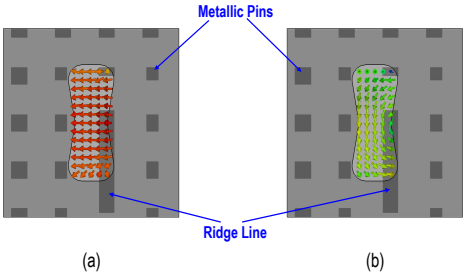

Figure 4.8: Illustrations for field-distributions: (a) E-filed. (b) H-field.

slot. This method is actually a magnetic coupling radiation, which is different from excitation method stated in. It avoids utilization of the conventional bend ridge line and makes the feed network very compact so the layout of the feed network is possible in such limited space as in the single-layered corporate-feed network case. The length of the slot L_s is firstly chosen so that the mutual coupling to the neighbor feed line can be eliminated. If L_s is small, the slot would not extend to the neighbor ridge feed line. W_1, W_2, H_s and L_r have been optimized to achieve the minimum reflection coefficient.

Table 4.2: Geometrical Parameters of 2×2 Unit Cell the Structure in Figure 4.7

	W_1	W_2	L_s	L_r	a_s	H_s	H_c
Geometries	1.13 mm	0.8 mm	2.7 mm	1.8 mm	0.3 mm	0.75 mm	1.25 mm

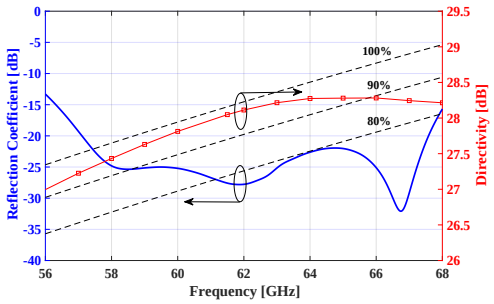

Figure 4.9: Simulated reflection coefficient of the single slot unit cell and directivity of an array antenna with 8×8 slot aperture dimension in infinite array environment.

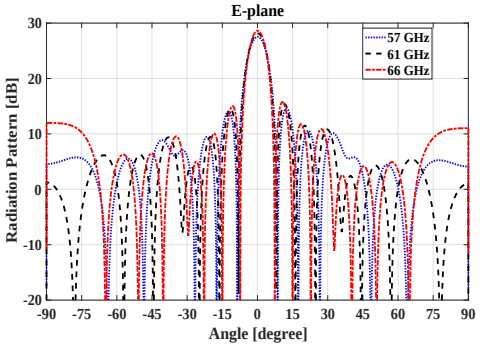

Figure 4.10: E-plane radiation pattern of the 8×8-element array antenna with periodic boundary condition.

Table 4.2 lists the optimized geometrical parameters of the unit cell shown in Figure 4.7. Figure 4.8 depicts the corresponding E- and H-fields distributions in the double ridged slot from CST Microwave Studio. The magnetic field is desired as predicted before. The distance between any two slots is equal to $0.87\lambda_0$, which satisfies the condition of non-grating lobes (element spacing $d<1/(1+1/8)\lambda_0=0.89\lambda_0$) in both E- and H-planes. Figure 4.9 shows corresponding reflection coefficient of the unit cell and the directivity of 8×8-element array antenna in infinite array environment. It has 20% impedance bandwidth (over 56-68 GHz) with input reflection coefficient better than -15 dB. The directivity is higher than 27.5 dBi and the aperture efficiency is better than 90% from 56 to 66 GHz. Here we have utilized the CST Microwave Studio periodic boundary condition along the lateral and longitudinal directions of 8×8-element in order to estimate the radiation pattern of the whole structure. Figure 4.10 and 4.11 illustrate the radiation patterns in both E- and H-planes of 8 ×8-element slot array antenna.

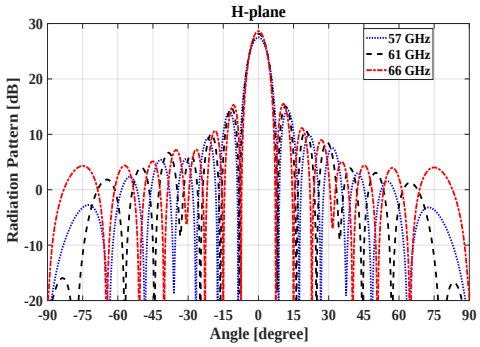

Figure 4.11: H-plane radiation pattern of the 8×8-element array antenna with periodic boundary condition.

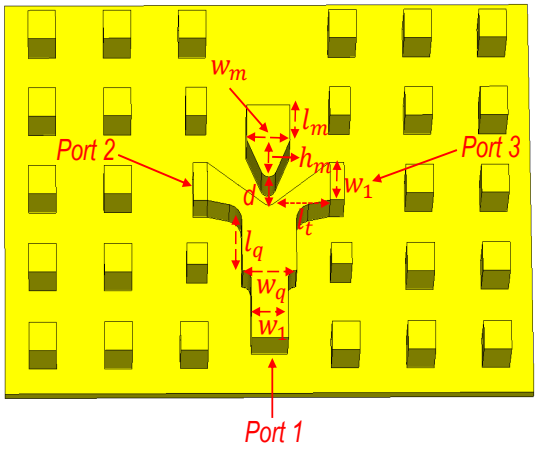

Figure 4.12: Geometry of the T-junction power divider based on RGW in this work. The upper metallic plate is hidden.

4.4 Corporate-Feed Network Design

The corporate-feed array antenna utilizes a T-junction power divider to feed each unit cell in the whole array antenna. The configuration of the T-junction RGW power divider used in this work is depicted in Figure 4.12. In Table 4.3, the geometrical parameters of the T-junction RGW power divider are listed. The corresponding simulated reflection coefficient is shown in Figure 4.13, which is below -30 dB from

Table 4.3: Design Parameters of the Structure in Figure 4.12

	W_1	W_q	l_q	l_t	d	w_m	l_m	h_m
Geometries	0.54 mm	0.8 mm	0.72 mm	0.92 mm	0.4 mm	0.72 mm	0.6 mm	0.47 mm

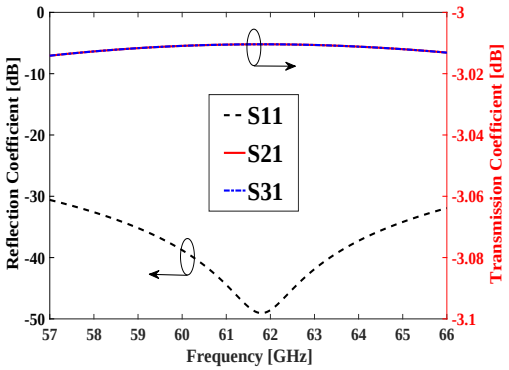

Figure 4.13: Simulated reflection coefficient and transmission coefficient of the power divider in Figure 4.12.

57 to 66 GHz. In order to have an easy massive production of the antenna by using molding technique of plastic material with metalized surface treatment, the smallest dimensions of the extruding parts (pins and ridges) are 0.4 mm.

The whole array antenna in this work is excited through a standard V-band rectangular waveguide (WR-15) at the bottom of whole structure. In this work we prefer a hybrid power divider similar as that described. The hybrid structure is illustrated in Figure 4.14. The simulated S-parameters of the structure both in amplitude and phase are shown in Figure 4.15. The reflection coefficient S_{11} in the whole band 56 – 68 GHz is below -20 dB. In addition, we should point out that the phases of the output ports have 180 degree difference, as shown in Figure 4.15 (b). Figure 4.16 shows the whole array antenna. The complete corporate-feed network consists of two 16-way RGW power dividers from central hybrid transition power

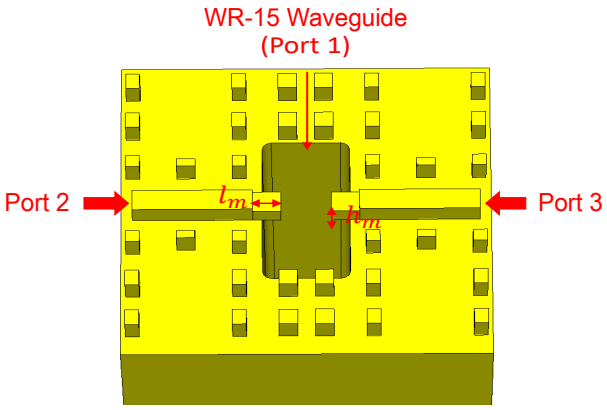

Figure 4.14: Geometrical illustration for hybrid transition from WR-15 to RGW. l_m = 0.75 mm and h_m = 0.45 mm.

divider to 64 radiating slots. The two 16-way feed networks are mirrored since the phase difference from hybrid transition part is able to be compensated. The thickness of the whole array antenna is 9.7 mm.

4.5 Experimental Results

The fabricated 8×8 slot array antenna is illustrated in Figure 4.17. The prototype is manufactured by Computerized Numerical Control (CNC) technology with aluminium (with electric conductivity 3.6 × 10^7 S/m). Planar dimension of the proposed antenna is 36 mm × 36 mm (The dimensions of effective aperture are 33.6 mm × 33.6 mm).

The entire structure is simulated in CST Microwave Studio. Since the hybrid transition, T-junction power divider and unit cell already have excellent reflection coefficients, the simulated reflection coefficient of complete antenna is below -15 dB from 57 to 66 GHz without any further optimization, as shown in Figure 4.18. However, the measured reflection coefficient is a bit higher than simulated one because the assembly tolerance of the proposed antenna is around 0.015 mm, which is measured by a X-ray inspection machine of Nikon, XTH 160 with a measurement tolerance of 20 nm.

The radiation patterns and the gain were measured in an anechoic chamber in China Academy of Space Technology in Shanghai. The simulated and the measured far-field radiation patterns of proposed antenna at 57, 62 and 67 GHz in both E- and H-planes are depicted in Figure 4.19. The measured radiation patterns show a good agreement with the simulated results. The simulated and the measured radiation patterns are symmetrical, and the first relative side-lobe levels in both E- and H-planes are around -12 dB. These mean that the distribution network works very well

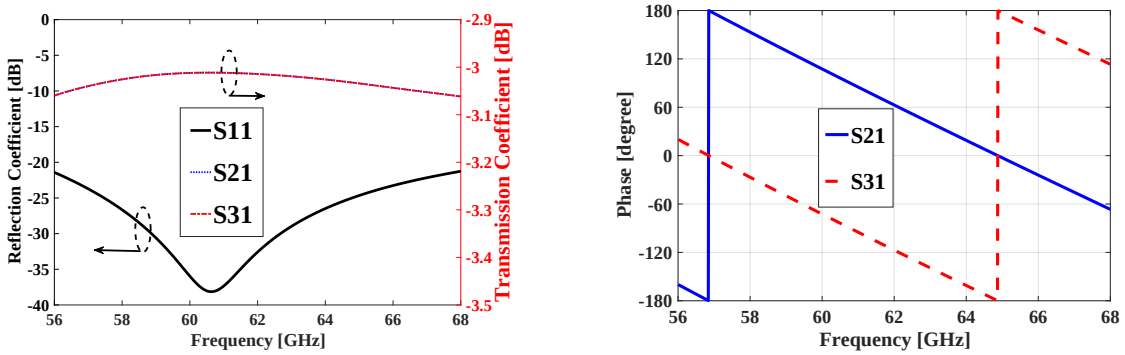

(a) (b)

Figure 4.15: Simulated S-parameter results of designed hybrid transition from WR-15 to RGW. (a) Amplitude. (b) Phase.

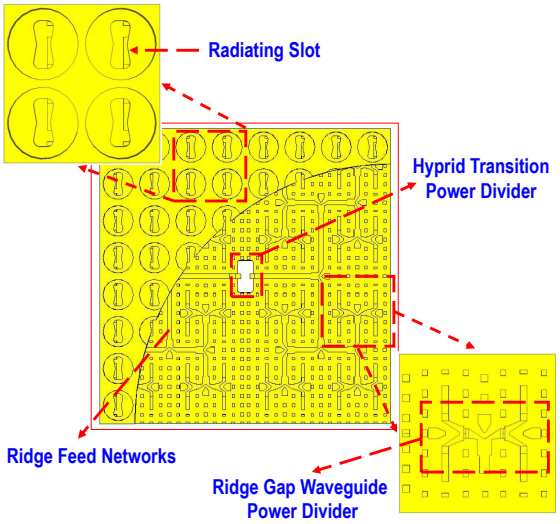

Figure 4.16: Proposed single-layered corporate-feed 8×8 slot array antenna.

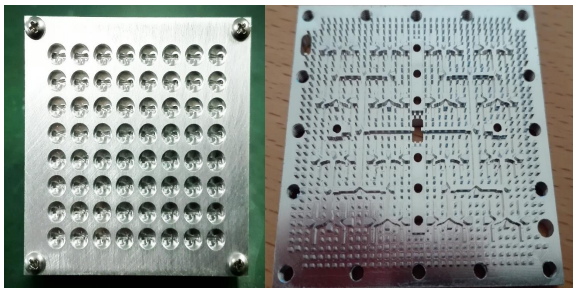

Figure 4.17: Configuration of the 8×8 slot array and photos of the fabricated antenna.

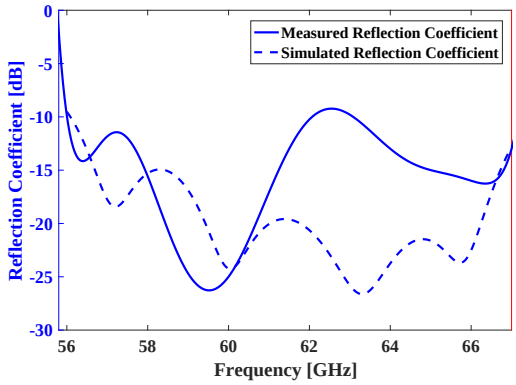

Figure 4.18: The simulated and the measured reflection coefficients of the proposed array antenna.

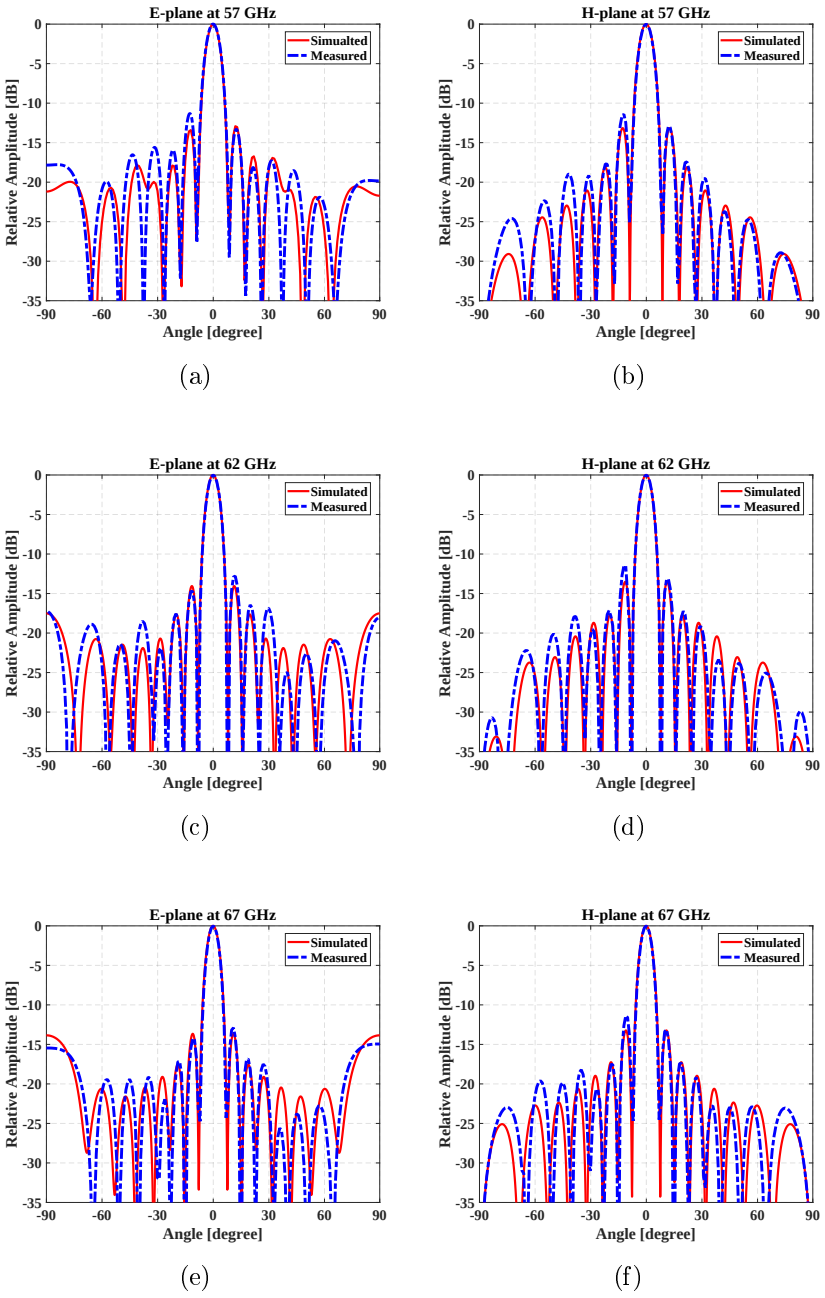

Figure 4.19: The simulated and the measured radiation patterns of proposed array antenna on both E-plane and H-plane at 57 GHz, 62 GHz and 67 GHz.

with low mutual couplings among the ridge feed lines. Since the element spacing of proposed antenna is 4.2 mm and wavelength at 67 GHz is equal to 4.477 mm, so the ratio 4.2/4.477= 0.94, which is larger than the non-grating lobes condition of 0.89 at 67 GHz, the radiation patterns in E-plane at 67 GHz at $\pm$ 90 degree are higher than the desired.

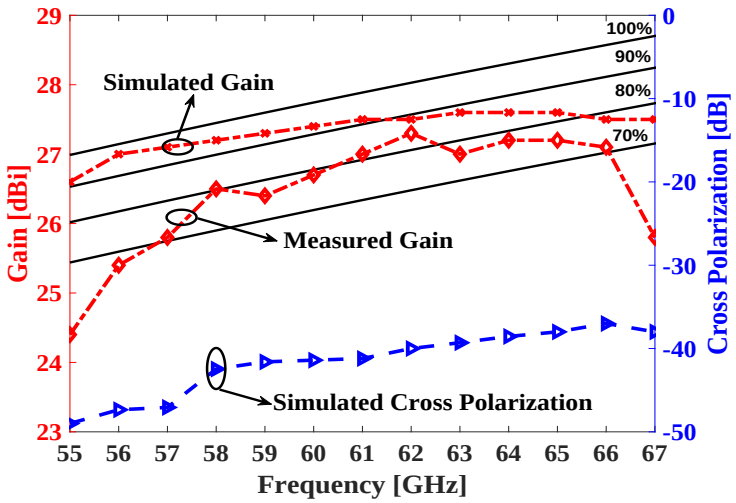

Figure 4.20: Red lines: simulated and measured gains of the proposed array antenna. Blue line: simulated cross-polarized value.

The measured and the simulated antenna gains are shown in Figure 4.20. It can be observed that the realized gain varies from 25.8 to 27 dBi over 57 to 66 GHz, whereas the antenna efficiency is more than 70% (Here the definition of antenna efficiency is defined as e_{ant}=e_{rad}·e_{pol}·e_{ap}, where e_{rad}, e_{pol} and e_{ap} are radiation efficiency, polarization efficiency and aperture efficiency, respectively). The simulated relative cross-polarization values are below -37 dB from 56 to 67 GHz, as also seen in Figure 4.20.

Conclusion

A single-layered corporate-feed array antenna based on RGW at 60-GHz is presented. This array antenna not only overcomes the disadvantage of narrow bandwidth from conventional single layer array with series-fed network, but also realize the advantage of wideband from three-layer slot array with backed cavity. The simpler geometry will definitely decrease the manufacture cost so that it has huge commercial potential in the future. The array antenna can be directly connected with standard WR-15 interface. An 8×8-element slot array has been designed, simulated, manufactured and measured. The measured gain is higher than 26 dBi from 58 to 66 GHz, correspondingly the antenna efficiency larger than 70%.

Chapter 5

Design and Fabrication of a High-Gain Slot Array Antenna based on Ridge Gap Waveguide at 140 GHz

This paper presents a new design of slot array antenna based on ridge gap waveguide at 140 GHz. The proposed array antenna consists of 32×32 radiation slots, backed cavities and full-corporate distribution network based on ridge gap waveguide. In order to fabricate the proposed array antenna by Computerized Numerical Control (CNC) technology, the periodic pin structure has been chosen with an aspect ratio of 1.5:1. Since the layout space for distribution networks is very limited, a novel stepped T-junction power divider is introduced in this work. The achieved reflection coefficient is much lower than that of the previous continuous T-junction power dividers which enables easy cascading of several T-junctions for building up a very large feed network. The measured results demonstrate about 11.4% of reflection coefficient bandwidth (|S11| < -10 dB) covering the 135—151 GHz frequency range, and the measured gain is larger than 37 dBi over the band with more than 50% antenna efficiency.

5.1 Introduction

Recently, D-band (110-170 GHz) has gained lots of attention for wireless applications, such as radar and wireless communication systems. As seen in Figure 5.1, the frequency band 135-155 GHz has the lowest air attenuation over the whole D-band. It is very advantageous to utilize this frequency band for high data rate wireless links. Due to several limitations in commercially available D-band electronics such as output power, Local oscillator leakage and packaging losses, the high-gain and high-efficiency antenna plays a very important role for the point-to-point wireless links. Usually, a parabolic reflector antenna is a classic choice for such a radio links system. However,

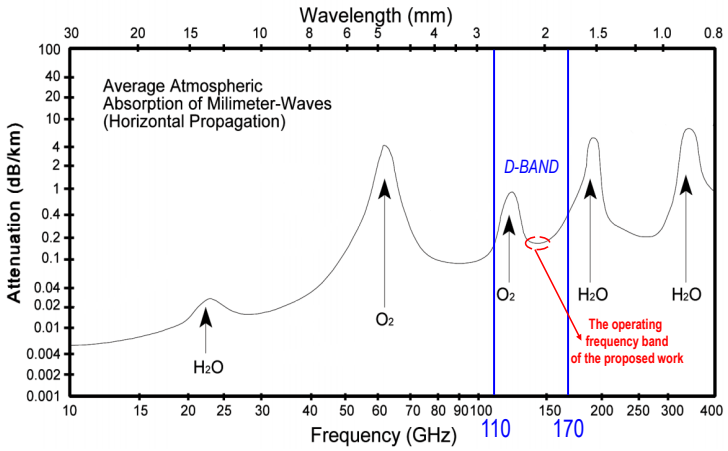

Figure 5.1: Average atmospheric absorption of millimeter-waves at sea level.

such a bulky dimension makes it not convenient for integration with front-end planar circuits. Hollow waveguide slot array antenna is probably another option. However, the diffusion bonding technology needs around 1000^oC with precise thermal control and high mechanical pressure which makes this technology rather expensive. In past few years, substrate integrated waveguide (SIW) and its applications for array antennas have been explored. However, the substrate is a fundamental component and its dielectric loss is becoming problematically significant versus the frequency.

In this chapter, we present a slot array antenna based on ridge gap waveguide at 140 GHz. The major challenges are stated as follows. The pin dimensions significantly decrease up to that level which becomes very challenging to fabricate by using conventional CNC milling or molding technique. The pins size had been chosen as $0.4\times0.4\ mm^2$ with an aspect ratio of 3.25:1 in the every slot array antenna. In this chapter, relatively larger pins are selected for 140 GHz array antenna so that the fabrication technology such as the CNC milling can be used for fabricating the antenna. Secondly, the conduction loss at 140 GHz becomes much greater then that of lower frequency band because of the skin effect and surface roughness. Thereby, the insertion losses of the sub-array, T-junction power divider and the other transition parts should be minimized so that the antenna efficiency is guaranteed. This high-gain antenna could be an alternative to reflector, lens or slot array by diffusion bonding technology in wireless link systems.

5.2 Antenna Design

5.2.1 Design for Sub-Array

According to the former discussion in Chapter 1, an arbitrary gap waveguide is able to provide a stopband over a specific frequency range between the two plates of Perfect Electric Conductor(PEC) and Perfect Magnetic Conductor (PMC). Since our design target is from 135-150 GHz, the dimensions of metallic pins are theoretically smaller than 0.15 mm according to the previous experience. The width of the metallic pins are appropriately selected in this work so that the proposed array antenna is able to be fabricated by CNC milling technology. A center frequency of $f_0 = 140$ GHz is assumed in this work. Then the height of the pins is determined as $\lambda_0/4$, which is equal to 2.2 mm. Thereby, the height of metallic pins is selected as $h = 0.58$ mm in this work. Furthermore, for achieving good radiation patterns the spacing between any two slots is selected as 1.8 mm, which is equal to $0.81\lambda_0$. Having considered the layout of the distribution network, five rows of metallic pins are required for the dimension of 3.6 mm and the corresponding periodicity of metallic pins is 0.72 mm. The dispersion diagram of the ridge gap waveguide is depicted in Figure 5.3. The obtained stopband is from 100 to 180 GHz, which covers our design target 135-150 GHz. The corresponding geometrical parameters of the proposed RGW are listed in Table 5.1.

As illustrated in Figure 5.4, the configuration of a 2×2-element sub-array is first designed using periodic boundary condition in CST Microwave Studio. The top of the entire sub-array is the radiation layer, which contains radiation slots with rectangular flare. The function of the flared slot is to suppress mutual coupling between slots and improve the bandwidth of the sub-array. Just below the slot layer, a gap waveguide cavity layer is placed. The electromagnetic coupling to the cavity through a hole

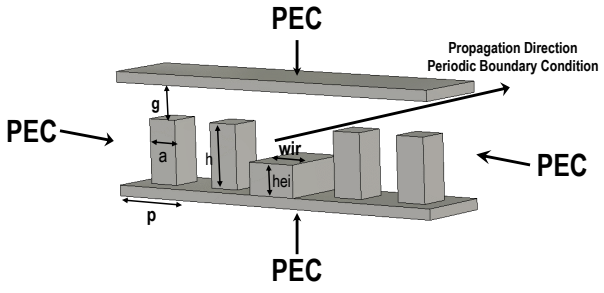

Figure 5.2: Infinite periodic unit cell based on RGW structure.

Table 5.1: Design Parameters of the Structure in Figure 5.2

	wir	*hei*	*p*	*h*	*d*	*a*	*g*
Geometries	0.45 mm	0.3 mm	0.72 mm	0.58 mm	0.35 mm	0.38 mm	0.05 mm

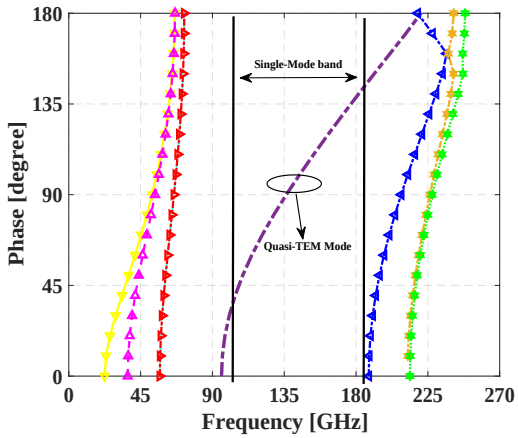

Figure 5.3: Dispersion diagram for the infinite periodic unit cell including a ridge in RGW.

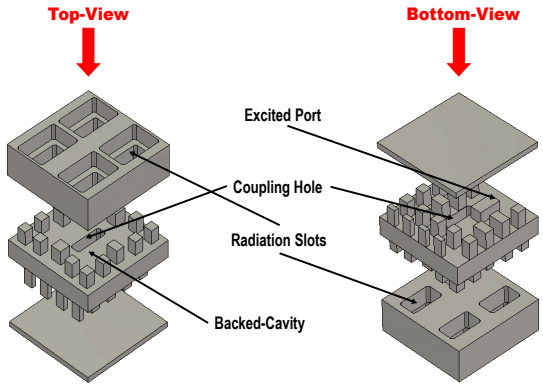

Figure 5.4: Distributed view of the proposed 2×2 cavity-backed slot sub-array.

aperture, which is excited via a ridge gap waveguide feeding line. The distribution network is placed on the back side of the cavity layer. The major reason for this design is to reduce the misalignment error between the separate cavity layer and the feed layer which becomes very tricky at D-band and which effects the operating bandwidth of the sub-array used previously. Thereby, the bottom waveguide layer is a smooth metallic plate. Because all three layers are separated by a small gap, there

Table 5.2: Design Parameters of the Structure in Figure 5.2

	W	d	$Ls1$	$Ws1$	$Ls2$	$Ws2$	Wb
Geometries	3.6 mm	1.8 mm	1.75 mm	1.15 mm	1.4 mm	0.72 mm	2.59 mm
	Lb	Wr	Lr	Wc	Lc	Wp	Lri
Geometries	2.68 mm	0.45 mm	0.46 mm	0.4 mm	1.32 mm	0.55 mm	0.81 mm

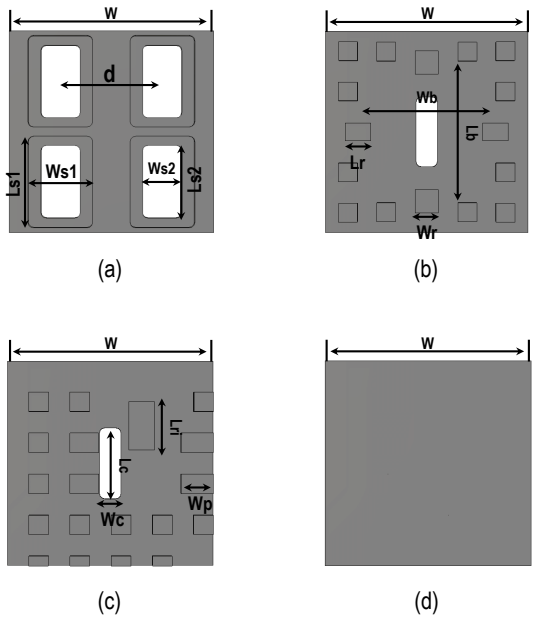

Figure 5.5: Geometrical parameters of a 2×2 slots array. (a) Top radiation slots layer. (b) Backed cavity layer. (c) Distribution network layer. (d) Bottom metallic layer.

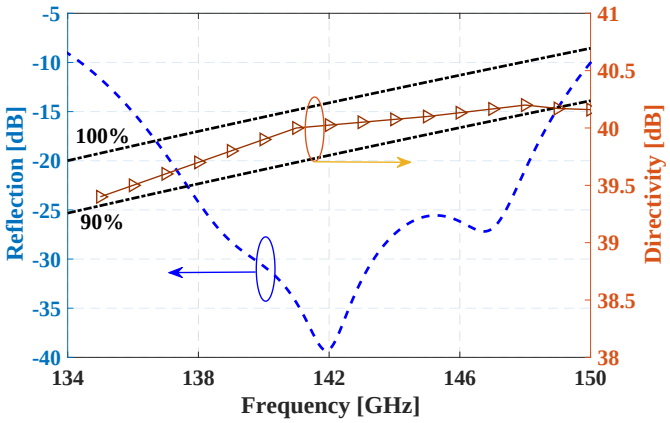

Figure 5.6: Simulated directivity and reflection coefficient of the 2×2 sub-array.

is no electrical contact between the different layers. The designed sub-array is 3.6 mm × 3.6 mm in both E- and H-planes. Figure 5.5 illustrates the detailed geometrical parameters of the 2×2 sub-array, and the corresponding values are listed in Table 5.2. The geometry is optimized by setting periodic boundary conditions in the CST Microwave Studio. In Figure 5.6, the blue line shows the reflection coefficient, and an

11.5% impedance bandwidth (over 134-150 GHz) with the input reflection coefficient below -10 dB is achieved. The yellow line with triangle marks depicts the simulated directivity of the 32×32 slot array in infinite array environment. The simulated antenna efficiency is higher than 90% from 135 to 148 GHz.

5.2.2 Design for Distribution Networks

T-junction power divider on RGW in the V-band have been explored very well. Because the periodic length p is selected as 1.1 mm and a as 0.4 mm in the previous design of V-band, there are enough space for the layout of the bend ridges. In this work, the periodic length is so small that the T-junction power divider with continuous bend ridge is impossible to fit in. For this reason, we have developed a stepped T-junction power divider, as depicted in Figure 5.7. In Table 5.3, the geometrical parameters of the T-junction RGW power divider are listed. The corresponding simulated reflection coefficient is shown in Figure 5.8, which is below -40 dB from 134 to 152 GHz. This performance is much better than the previous designs. Furthermore, it is easy to be fabricated so that it can be found more applications in the other frequency bands. The whole array antenna in this paper is excited through a standard D-band rectangular waveguide (WR-6) at the bottom of the whole structure. Then, a hybrid power divider is designed, and its geometry is illustrated in Figure 5.9. The simulated S-parameters of the structure both in amplitude and phase are shown in Figure 5.10. The reflection coefficient is below -27 dB in the whole band 134-150 GHz. The corresponding design parameters are listed in Table 5.3. In addition, such a hybrid structure is essentially a differential feeding geometry so that the phases of the output ports have 180 degree difference, as shown in Figure 5.10(b). In order to

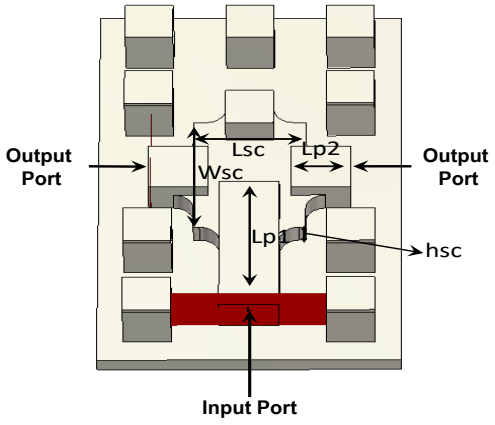

Figure 5.7: Geometry of the discontinuous T-junction power divider based on RGW in this work. The upper metallic plate is hidden.

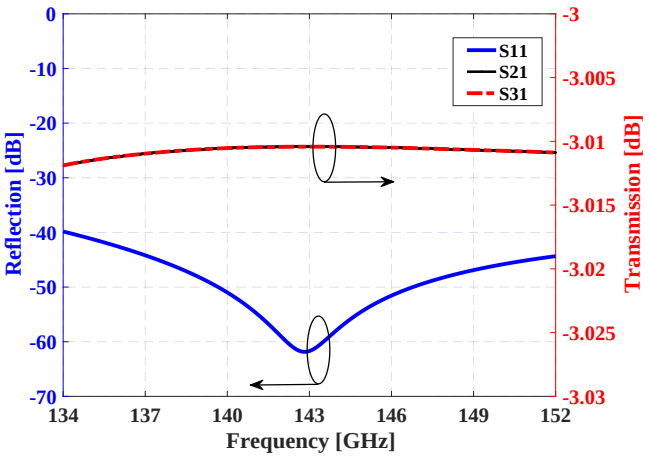

Figure 5.8: Simulated reflection coefficient and transmission coefficient of the power divider in Figure 5.7.

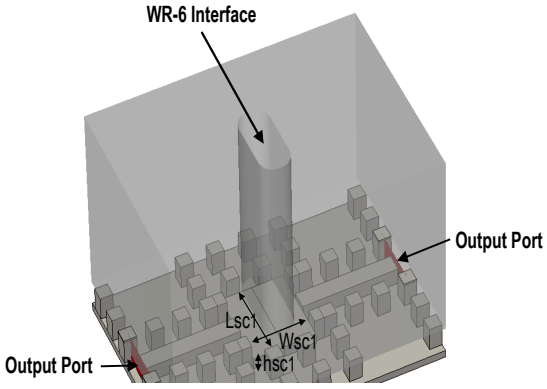

Figure 5.9: Geometrical illustration for hybrid transition from WR-6 to RGW.

compensate the difference of the output phases, the two distribution networks are in a mirror geometry. The final numerical designed antenna is shown in Figure 5.11. The thickness of the whole array antenna is 7.7 mm.

5.3 Experimental Results

The fabricated prototype of the 32×32 slot array antenna has been done by DMG MORI CNC Milling machine with aluminum (with electric conductivity 3.6×10^7 S/m), which is illustrated in Figure 5.12. The manufacture tolerance of the machine is 1 μm, which is accurate enough for the designed antenna. The planar dimension of

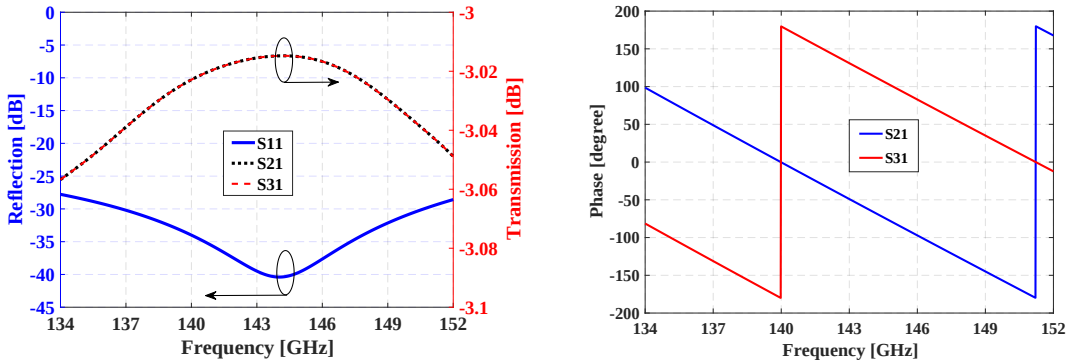

(a) (b)

Figure 5.10: Simulated S-parameter results of designed hybrid transition from WR-6 to RGW. (a) Amplitude. (b) Phase.

Table 5.3: DESIGN PARAMETERS OF THE STRUCTURES IN FIGURE 5.7 AND FIGURE 5.9

$Lp1$	1.35 mm
hsc	0.27 mm
Wsc	1.16 mm
Lsc	0.84 mm
$Lp2$	0.45 mm
$Lsc1$	2.05 mm
$Wsc1$	1.77 mm
$hsc1$	0.30 mm

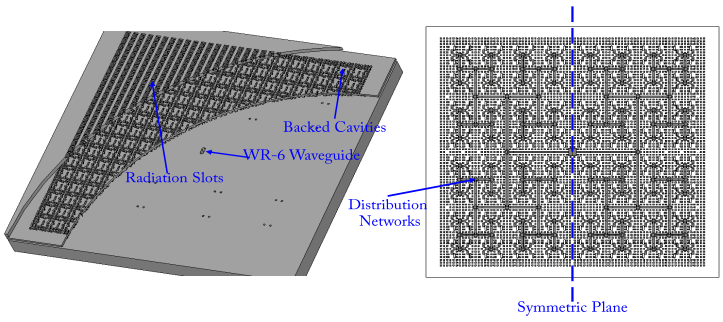

Figure 5.11: The proposed 32×32 slot array antenna and its full corporate-feed distribution networks.

the proposed antenna is 65 mm × 65 mm (the dimensions of effective aperture are 57.6 mm×57.6 mm). The entire structure is simulated in CST Microwave Studio, and

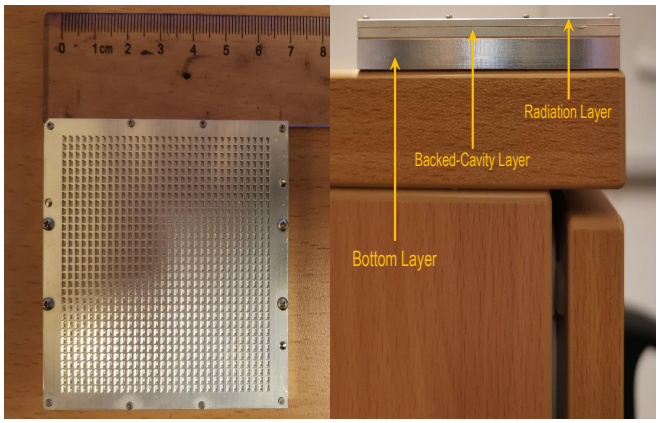

Figure 5.12: Photograph of the final fabricated 32× 32 slot array antenna.

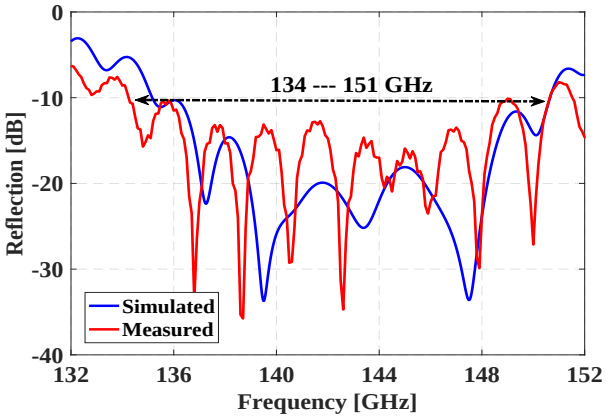

Figure 5.13: Simulated and the measured reflection coefficients of the proposed array antenna.

the simulated reflection coefficient of the completed antenna is below -10 dB from 135 to 150 GHz without any further optimization, as shown in Figure 5.13. Nevertheless, the measured one is a bit higher than the simulated one. The misalignment of three antenna layers from assembling is always a problem for such a high frequency band. In addition, the extra ohmic losses caused by ridge surface roughness from CNC milling fabrication should be also considered for the difference of reflections. The radiation patterns and the gain were measured by a near-field measurement setup in an anechoic chamber at Southeast University in Nanjing, China, as shown in Figure 5.14. The simulated and the measured radiation patterns of the fabricated antenna at 135, 140, 145 and 150 GHz in both E- and H-planes are depicted in Figure 5.15 and Figure 5.16. The measured radiation patterns have reasonable agreements with

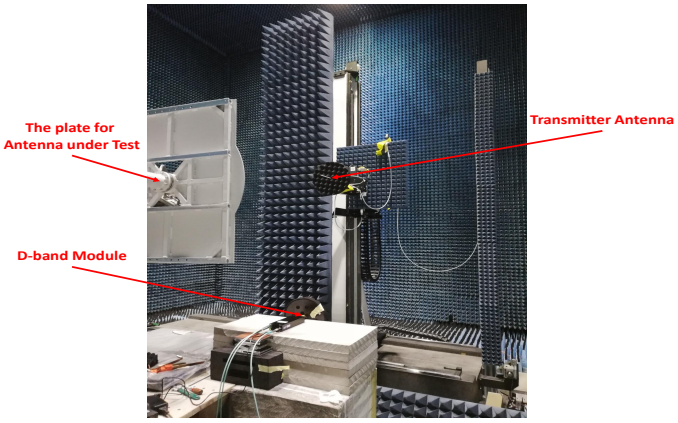

Figure 5.14: Photograph of the measurement setup for the gain and the radiation pattern test.

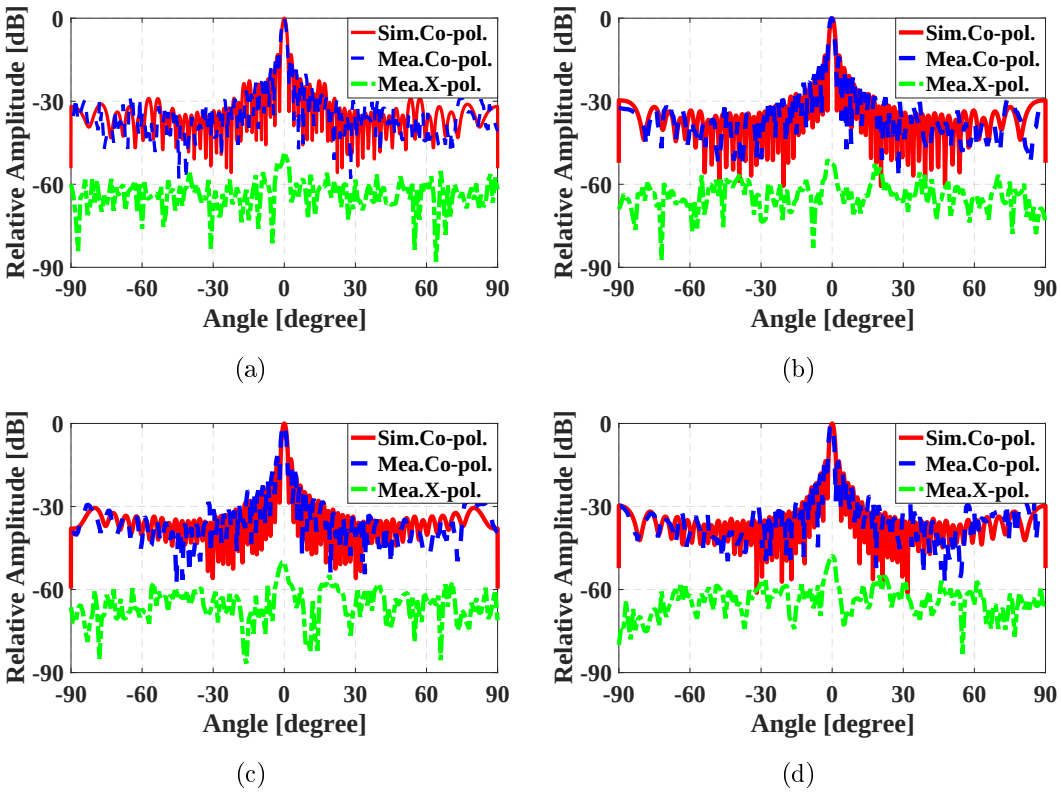

Figure 5.15: The simulated and the measured radiation patterns of proposed array antenna on E-plane at (a) 135 GHz, (b) 140 GHz, (c) 145 GHz and (d) 150 GHz.

the simulated ones while the measured side lobes are a little bit higher than simulated ones. Nevertheless, the measured radiation patterns are symmetrical, and their first side lobes both in E- and H-planes are lower than -13 dB. The measured gain is higher than 37 dBi with the measured antenna efficiency higher than 50% from 136 to 150

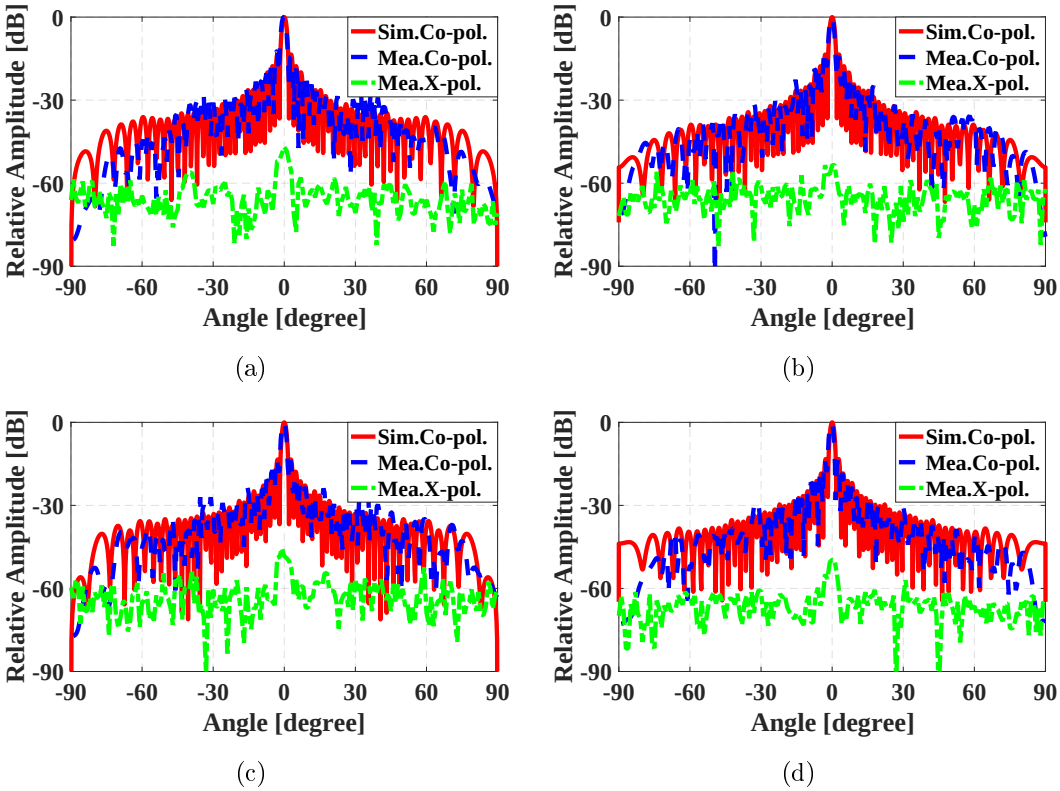

Figure 5.16: The simulated and the measured radiation patterns of proposed array antenna on H-plane at (a) 135 GHz, (b) 140 GHz, (c) 145 GHz and (d) 150 GHz.

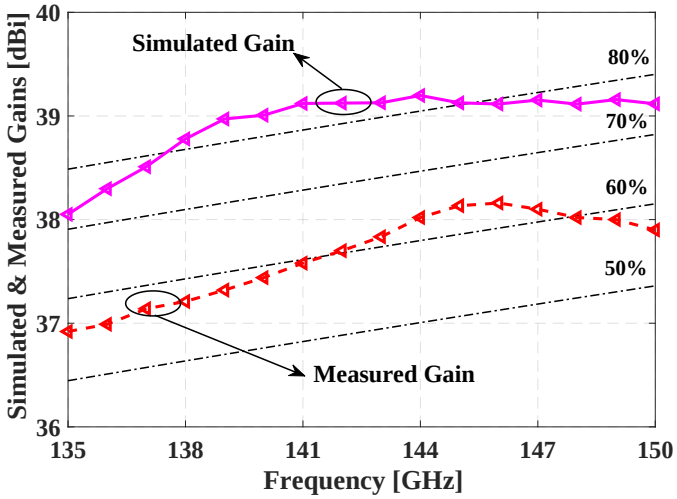

Figure 5.17: Simulated and measured gains of the proposed array antenna.

GHz, as depicted in Figure 5.17. There are big differences between the measured and the simulated gains in the whole frequency band. In this chapter, we have realized a slot array antenna based on RGW with low cost, high-gain, high-efficiency and low profile. This type of slot array antenna is very practical for D-band high speed wireless links.

5.4 Conclusion

A 32×32 corporate-feed array antenna based on RGW in D-band is presented in this work. The simpler geometry will definitely decrease the manufacturing cost so that it has huge commercial potential in the future. The array antenna can be directly connected with standard WR-6 interface. The measured gain is higher than 37 dBi from 135 to 150 GHz, correspondingly the antenna efficiency larger than 50%.

Chapter 6

Summary and Conclusion

As a newly invented waveguide geometry, gap waveguide technology is able to overcome the limitations of the traditional transmission lines, such as microstrip, coplanar waveguide and rectangular hollow waveguide. Especially, gap waveguide shows very strong competitive strength from Ka- to D-band, such as low loss and flexible fabrication and assembly. This thesis presents several types of the slot array antennas fed by inverted microstrip gap waveguide, ridge gap waveguide and groove gap waveguide. Furthermore, gap waveguide also shows advantages in passive components, MMIC packaging and achievements in integration of active components in millimeter-wave frequency bands. Moreover, the realization of gap waveguide structures is explored by using several different fabrication methods, such as die-sink EDM, CNC micromachining and micro-molding. The first part of this thesis comprises an introduction of gap waveguide theory, the slot array antenna designed by gap waveguide geometry from V-band to D-band. From the measurement results, gap waveguide structure shows big advantages over the traditional hollow waveguide and microstrip line. It is very helpful for industrial applications in future. The second part of the thesis consists of the research contributions by the author, and this section summarizes those appended articles.

References

[1] P. Smulders, "Exploiting the 60 ghz band for local wireless multimedia access: Prospects and future directions," *IEEE Communications Magazine*, vol. 40, no. 1, pp. 140–147, 2002.

[2] L. Lin and Z. Li, "Study of transmission effects of millimeter wave through fog and haze," in *2016 IEEE Advanced Information Management, Communicates, Electronic and Automation Control Conference (IMCEC)*. IEEE, 2016, pp. 1591–1596.

[3] D. Deslandes and K. Wu, "Integrated microstrip and rectangular waveguide in planar form," *IEEE Microwave and Wireless Components Letters*, vol. 11, no. 2, pp. 68–70, 2001.

[4] F. Xu and K. Wu, "Guided-wave and leakage characteristics of substrate integrated waveguide," *IEEE Transactions on Microwave Theory and Techniques*, vol. 53, no. 1, pp. 66–73, 2005.

[5] L. Wang, X. Yin, S. Li, H. Zhao, L. Liu, and M. Zhang, "Phase corrected substrate integrated waveguide h-plane horn antenna with embedded metal-via arrays," *IEEE Transactions on Antennas and Propagation*, vol. 62, no. 4, pp. 1854–1861, April 2014.

[6] T. Li and Z. N. Chen, "Control of beam direction for substrate-integrated waveguide slot array antenna using metasurface," *IEEE Transactions on Antennas and Propagation*, vol. 66, no. 6, pp. 2862–2869, June 2018.

[7] L. Wang, X. Yin, M. Esquius-Morote, H. Zhao, and J. R. Mosig, "Circularly polarized compact ltsa array in siw technology," *IEEE Transactions on Antennas and Propagation*, vol. 65, no. 6, pp. 3247–3252, June 2017.

[8] T. Li and Z. N. Chen, "Wideband substrate-integrated waveguide-fed endfire metasurface antenna array," *IEEE Transactions on Antennas and Propagation*, vol. 66, no. 12, pp. 7032–7040, Dec 2018.

[9] D. Guan, C. Ding, Z. Qian, Y. Zhang, Y. Jay Guo, and K. Gong, "Broadband high-gain siw cavity-backed circular-polarized array antenna," *IEEE Transactions on Antennas and Propagation*, vol. 64, no. 4, pp. 1493–1497, April 2016.

[10] S. E. Hosseininejad and N. Komjani, "Optimum design of traveling-wave siw slot array antennas," *IEEE Transactions on Antennas and Propagation*, vol. 61, no. 4, pp. 1971–1975, April 2013.

[11] Z. Hao, Q. Yuan, B. Li, and G. Q. Luo, "Wideband w-band substrate-integrated waveguide magnetoelectric (me) dipole array antenna," *IEEE Transactions on Antennas and Propagation*, vol. 66, no. 6, pp. 3195–3200, June 2018.

[12] J. Xiao, Z. Qi, X. Li, and H. Zhu, "Broadband and high-gain siw-fed slot array for millimeter-wave applications," *IEEE Transactions on Antennas and Propagation*, vol. 67, no. 5, pp. 3484–3489, May 2019.

[13] M. Bozzi, A. Georgiadis, and K. Wu, "Review of substrate-integrated waveguide circuits and antennas," *IET Microwaves, Antennas Propagation*, vol. 5, no. 8, pp. 909–920, June 2011.

[14] M. Bozzi, L. Perregrini, and K. Wu, "Modeling of conductor, dielectric, and radiation losses in substrate integrated waveguide by the boundary integral-resonant mode expansion method," *IEEE Transactions on Microwave Theory and Techniques*, vol. 56, no. 12, pp. 3153–3161, Dec 2008.

[15] D. Deslandes and Ke Wu, "Accurate modeling, wave mechanisms, and design considerations of a substrate integrated waveguide," *IEEE Transactions on Microwave Theory and Techniques*, vol. 54, no. 6, pp. 2516–2526, June 2006.

[16] P.-S. Kildal, E. Alfonso, A. Valero-Nogueira, and E. Rajo-Iglesias, "Local metamaterial-based waveguides in gaps between parallel metal plates," *IEEE Antennas and Wireless Propagation Letters*, vol. 8, pp. 84–87, 2009.

[17] P.-S. Kildal, "Artificially soft and hard surfaces in electromagnetics," *IEEE Transactions on Antennas and Propagation*, vol. 38, no. 10, pp. 1537–1544, 1990.

[18] J. Liu, J. Yang, and A. U. Zaman, "Analytical solutions to characteristic impedance and losses of inverted microstrip gap waveguide based on variational method," *IEEE Transactions on Antennas and Propagation*, vol. 66, no. 12, pp. 7049–7057, Dec 2018.

[19] H. Raza, J. Yang, P. Kildal, and E. Alfonso Alos, "Microstrip-ridge gap waveguide-study of losses, bends, and transition to wr-15," *IEEE Transactions on Microwave Theory and Techniques*, vol. 62, no. 9, pp. 1943–1952, Sep. 2014.

[20] M. Ferrando-Rocher, J. I. Herranz-Herruzo, A. Valero-Nogueira, and B. Bernardo-Clemente, "Performance assessment of gap-waveguide array antennas: Cnc milling versus three-dimensional printing," *IEEE Antennas and Wireless Propagation Letters*, vol. 17, no. 11, pp. 2056–2060, Nov 2018.

[21] A. Vosoogh, M. S. Sorkherizi, V. Vassilev, A. U. Zaman, Z. S. He, J. Yang, A. A. Kishk, and H. Zirath, "Compact integrated full-duplex gap waveguide-based radio front end for multi-gbit/s point-to-point backhaul links at e-band," *IEEE Transactions on Microwave Theory and Techniques*, pp. 1–15, 2019.

[22] A. Vosoogh, A. Uz Zaman, V. Vassilev, and J. Yang, "Zero-gap waveguide: A parallel plate waveguide with flexible mechanical assembly for mm-wave antenna applications," *IEEE Transactions on Components, Packaging and Manufacturing Technology*, vol. 8, no. 12, pp. 2052–2059, Dec 2018.

[23] A. Farahbakhsh, D. Zarifi, and A. U. Zaman, "60-ghz groove gap waveguide based wideband h -plane power dividers and transitions: For use in high-gain slot array antenna," *IEEE Transactions on Microwave Theory and Techniques*, vol. 65, no. 11, pp. 4111–4121, Nov 2017.

[24] A. Vosoogh, M. S. Sorkherizi, A. U. Zaman, J. Yang, and A. A. Kishk, "An integrated ka-band diplexer-antenna array module based on gap waveguide technology with simple mechanical assembly and no electrical contact requirements," *IEEE Transactions on Microwave Theory and Techniques*, vol. 66, no. 2, pp. 962–972, Feb 2018.

[25] A. Vosoogh, A. Haddadi, A. U. Zaman, J. Yang, H. Zirath, and A. A. Kishk, "w-band low-profile monopulse slot array antenna based on gap waveguide corporate-feed network," *IEEE Transactions on Antennas and Propagation*, vol. 66, no. 12, pp. 6997–7009, Dec 2018.

[26] M. Al Sharkawy and A. A. Kishk, "Long slots array antenna based on ridge gap waveguide technology," *IEEE Transactions on Antennas and Propagation*, vol. 62, no. 10, pp. 5399–5403, Oct 2014.

[27] B. Cao, H. Wang, Y. Huang, and J. Zheng, "High-gain l-probe excited substrate integrated cavity antenna array with ltcc-based gap waveguide feeding network for w-band application," *IEEE Transactions on Antennas and Propagation*, vol. 63, no. 12, pp. 5465–5474, Dec 2015.

[28] A. Dadgarpour, M. S. Sorkherizi, T. A. Denidni, and A. A. Kishk, "Passive beam switching and dual-beam radiation slot antenna loaded with enz medium and excited through ridge gap waveguide at millimeter-waves," *IEEE Transactions on Antennas and Propagation*, vol. 65, no. 1, pp. 92–102, Jan 2017.

[29] D. Zarifi, A. Farahbakhsh, and A. U. Zaman, "A gap waveguide-fed wideband patch antenna array for 60-ghz applications," *IEEE Transactions on Antennas and Propagation*, vol. 65, no. 9, pp. 4875–4879, Sep. 2017.

[30] M. Sharifi Sorkherizi, A. Dadgarpour, and A. A. Kishk, "Planar high-efficiency antenna array using new printed ridge gap waveguide technology," *IEEE Transactions on Antennas and Propagation*, vol. 65, no. 7, pp. 3772–3776, July 2017.

[31] P. Sadri-Moshkenani, J. Rashed-Mohassel, and M. Shahabadi, "Microstrip antenna array fed by a low-loss gap-waveguide feed network," *IEEE Transactions on Antennas and Propagation*, vol. 66, no. 8, pp. 4359–4363, Aug 2018.

[32] A. Dadgarpour, M. Sharifi Sorkherizi, and A. A. Kishk, "Wideband low-loss magnetoelectric dipole antenna for 5g wireless network with gain enhancement using meta lens and gap waveguide technology feeding," *IEEE Transactions on Antennas and Propagation*, vol. 64, no. 12, pp. 5094–5101, Dec 2016.

[33] Y. Shi, W. Feng, H. Wang, W. Che, Q. Xue, J. Wang, J. Zhang, X. Qian, M. Zhou, and B. Cao, "Novel w -band ltcc transition from microstrip line to ridge gap waveguide and its application in 77/79 ghz antenna array," *IEEE Transactions on Antennas and Propagation*, vol. 67, no. 2, pp. 915–924, Feb 2019.

[34] E. Rajo-Iglesias, P. Kildal, A. U. Zaman, and A. Kishk, "Bed of springs for packaging of microstrip circuits in the microwave frequency range," *IEEE Transactions on Components, Packaging and Manufacturing Technology*, vol. 2, no. 10, pp. 1623–1628, Oct 2012.

[35] A. U. Zaman, M. Alexanderson, T. Vukusic, and P.-S. Kildal, "Gap waveguide pmc packaging for improved isolation of circuit components in high-frequency microwave modules," *IEEE Transactions on Components, Packaging and Manufacturing Technology*, vol. 4, no. 1, pp. 16–25, 2014.

[36] U. Nandi, A. U. Zaman, A. Vosoogh, and J. Yang, "Novel millimeter wave transition from microstrip line to groove gap waveguide for mmic packaging and antenna integration," *IEEE Microwave and Wireless Components Letters*, vol. 27, no. 8, pp. 691–693, Aug 2017.

[37] M. Sharifi Sorkherizi and A. A. Kishk, "Self-packaged, low-loss, planar bandpass filters for millimeter-wave application based on printed gap waveguide technology," *IEEE Transactions on Components, Packaging and Manufacturing Technology*, vol. 7, no. 9, pp. 1419–1431, Sep. 2017.

[38] A. U. Zaman, P. Kildal, and A. A. Kishk, "Narrow-band microwave filter using high-q groove gap waveguide resonators with manufacturing flexibility and no

sidewalls," *IEEE Transactions on Components, Packaging and Manufacturing Technology*, vol. 2, no. 11, pp. 1882–1889, 2012.

[39] M. S. Sorkherizi, A. Khaleghi, and P. Kildal, "Direct-coupled cavity filter in ridge gap waveguide," *IEEE Transactions on Components, Packaging and Manufacturing Technology*, vol. 4, no. 3, pp. 490–495, March 2014.

[40] A. A. Brazalez, A. U. Zaman, and P. Kildal, "Improved microstrip filters using pmc packaging by lid of nails," *IEEE Transactions on Components, Packaging and Manufacturing Technology*, vol. 2, no. 7, pp. 1075–1084, July 2012.

[41] B. Ahmadi and A. Banai, "Direct coupled resonator filters realized by gap waveguide technology," *IEEE Transactions on Microwave Theory and Techniques*, vol. 63, no. 10, pp. 3445–3452, Oct 2015.

[42] E. Pucci, E. Rajo-Iglesias, J.-L. Vazquez-Roy, and P.-S. Kildal, "Planar dual-mode horn array with corporate-feed network in inverted microstrip gap waveguide," *IEEE Transactions on Antennas and Propagation*, vol. 62, no. 7, pp. 3534–3542, 2014.

[43] A. Vosoogh, A. A. Brazalez, and P.-S. Kildal, "A v-band inverted microstrip gap waveguide end-coupled bandpass filter," *IEEE Microwave and Wireless Components Letters*, vol. 26, no. 4, pp. 261–263, 2016.

[44] S. A. Razavi, P.-S. Kildal, L. Xiang, H. Chen, and E. Alfonso, "Design of 60ghz planar array antennas using pcb-based microstrip-ridge gap waveguide and siw," in *8th European Conference on Antennas and Propagation (EuCAP), 2014*. Piscataway, NJ and Piscataway, NJ: IEEE, 2014, pp. 1825–1828.

[45] J. Liu, A. U. Zaman, and P.-S. Kildal, "Optimizing the numerical port for inverted microstrip gap waveguide in full-wave simulators," in *2016 10th European Conference on Antennas and Propagation (EuCAP)*. [Piscataway, New Jersey]: IEEE, 2016, pp. 1–5.

[46] A. A. Brazalez, E. Rajo-Iglesias, J. L. Vazquez-Roy, A. Vosoogh, and P.-S. Kildal, "Design and validation of microstrip gap waveguides and their transitions to rectangular waveguide, for millimeter-wave applications," *IEEE Transactions on Microwave Theory and Techniques*, vol. 63, no. 12, pp. 4035–4050, 2015.

[47] Y. Li and K.-M. Luk, "60-ghz substrate integrated waveguide fed cavity-backed aperture-coupled microstrip patch antenna arrays," *IEEE Transactions on Antennas and Propagation*, vol. 63, no. 3, pp. 1075–1085, 2015.

[48] J. Wu, Y. J. Cheng, and Y. Fan, "A wideband high-gain high-efficiency hybrid integrated plate array antenna for v-band inter-satellite links," *IEEE Transactions on Antennas and Propagation*, vol. 63, no. 4, pp. 1225–1233, 2015.

[49] Y. Miura, J. Hirokawa, M. Ando, Y. Shibuya, and G. Yoshida, "Double-layer full-corporate-feed hollow-waveguide slot array antenna in the 60-ghz band," *IEEE Transactions on Antennas and Propagation*, vol. 59, no. 8, pp. 2844–2851, 2011.

[50] D. Zarifi, A. Farahbakhsh, A. U. Zaman, and P.-S. Kildal, "Design and fabrication of a high-gain 60-ghz corrugated slot antenna array with ridge gap waveguide distribution layer," *IEEE Transactions on Antennas and Propagation*, vol. 64, no. 7, pp. 2905–2913, 2016.

[51] A. Vosoogh, P.-S. Kildal, and V. Vassilev, "Wideband and high-gain corporate-fed gap waveguide slot array antenna with etsi class ii radiation pattern in v -band," *IEEE Transactions on Antennas and Propagation*, vol. 65, no. 4, pp. 1823–1831, 2017.